cAMP-independent non-pigmentary actions of variant melanocortin 1 receptor: AKT-mediated activation of protective responses to oxidative DNA damage

María Castejón, Cecilia Herraiz[1], Conchi Olivares, Celia Jiménez-Cervantes and Jose Carlos García-Borrón

Department of Biochemistry, Molecular Biology and Immunology, School of Medicine, University of Murcia and Instituto Murciano de Investigacion Biosanitaria (IMIB).

[1] Corresponding author: Dr Cecilia Herraiz, ceciliahs@um.es. LAIB, Room 1.55. Campus de Ciencias de la Salud, Universidad de Murcia. Carretera Buenavista, s/n. 30120 El Palmar, Murcia, SPAIN.

Running title: cAMP-independent protective action of variant MC1R

Word count: Main text (Introduction, Results, Discussion and Methods): 4691 words (up to 4700 words allowed by the Editors)

Full text: 9484 words

Abstract

The melanocortin 1 receptor gene (*MC1R*), a well-established melanoma susceptibility gene, regulates the amount and type of melanin pigments formed within epidermal melanocytes. *MC1R* variants associated with increased melanoma risk promote production of photosensitizing pheomelanins as opposed to photoprotective eumelanins. Wild-type (WT) MC1R activates DNA repair and antioxidant defenses in a cAMP-dependent fashion. Since melanoma-associated *MC1R* variants are hypomorphic in cAMP signalling, these non-pigmentary actions are thought to be defective in *MC1R*-variant human melanoma cells and epidermal melanocytes, consistent with a higher mutation load in *MC1R*-variant melanomas. We compared induction of antioxidant enzymes and DNA damage responses in melanocytic cells of defined *MC1R* genotype. Increased expression of *catalase* (*CAT*) and *superoxide dismutase* (*SOD)* genes following MC1R activation was cAMP-dependent and required a WT MC1R genotype. Conversely, pretreatment of melanocytic cells with an MC1R agonist before an oxidative challenge with Luperox decreased i) accumulation of 8-oxo-7,8-dihydro-2'-deoxyguanine, a major product of oxidative DNA damage, ii) phosphorylation of histone H2AX, a marker of DNA double strand breaks and iii) formation of DNA breaks. These responses were comparable in cells WT for *MC1R* or harboring hypomorphic *MC1R* variants without detectable cAMP signalling. In *MC1R*-variant melanocytic cells, the DNA-protective responses were mediated by AKT. Conversely, in *MC1R*-WT melanocytic cells, high cAMP production downstream of MC1R blocked AKT activation and was responsible for inducing DNA repair. Accordingly, MC1R activation could promote repair of oxidative DNA damage by a cAMP-dependent pathway downstream of WT receptor, or via AKT in cells of variant *MC1R* genotype.

Keywords (3-6)

- melanocortin 1 receptor (MC1R)
- α melanocyte-stimulating hormone (α melanocortin; αMSH)
- oxidative DNA damage
- cAMP pathway
- AKT pathway
- melanoma

INTRODUCTION

The melanocortin 1 receptor (MC1R), a Gs protein-coupled receptor (GPCR) expressed by epidermal melanocytes, is critically involved in cutaneous responses to ultraviolet radiation (UVR)[1]. Solar UVR, the main external etiological factor for melanoma, causes DNA lesions directly or by oxidative processes triggered by UVR-induced reactive oxygen species (ROS). A causal link exists between UVR-induced DNA damage and skin carcinogenesis, particularly melanomagenesis[2–4]. Upon stimulation by keratinocyte-derived melanocortins, notably α melanocyte-stimulating hormone (αMSH), MC1R activates cAMP signalling to switch melanogenesis from basal synthesis of reddish pheomelanins to synthesis of darker eumelanins. Contrary to the well-established photoprotective effect of eumelanins, pheomelanins promote oxidative stress by UVR-dependent and independent mechanisms[5], thus acting as sensitizers that contribute to melanomagenesis[6]. Accordingly, dark-skinned individuals are less susceptible to sunburn and melanoma than people with pale skin.

Human *MC1R* (MIM#155555) is highly polymorphic, and almost 50% of individuals of Caucasian descent carry at least one variant allele[1,7,8]. Many *MC1R* polymorphisms are associated with pheomelanic pigmentation with red hair, fair skin, impaired tanning response to UVR and propensity to sunburn[9]. This phenotype, designated RHC, is also associated with skin cancer risk[10–12]. *MC1R* RHC alleles display hypomorphic signalling to the cAMP pathway[13–21]. The degree of functional impairment grossly correlates with penetrance, with strong R-type alleles such as R151C showing lower residual cAMP signalling than weaker "r-type" alleles[22].

Despite their photoprotective role, eumelanins only afford a moderate protection factor around 2-3 in darker-skinned individuals[23]. Moreover, a significant association of *MC1R* alleles and melanoma persists after stratification for pigmentation, pointing to pigment-independent actions of MC1R[24,25]. In *MC1R*-WT human melanocytes, αMSH enhances repair of UVR-induced cyclobutane pyrimidine dimers in a cAMP-dependent fashion[26,27]. Accordingly, it is believed that cAMP-dependent non-pigmentary actions including induction of antioxidant defenses and DNA repair contribute to the association of the *MC1R* genotype with melanoma[26–31].

Signalling downstream of MC1R is pleiotropic, with activation of mitogen-activated kinases ERK1/2 and the cAMP pathway[32]. In human melanocytes, ERK activation by MC1R relies on cAMP-independent transactivation of the cKIT tyrosine kinase receptor (RTK)[14,33,34]. Importantly, common R mutations impairing cAMP signalling have little effect on ERK activation downstream of MC1R[14,33,34], and their

possible effects on signalling to AKT remain largely unknown. Moreover, it has been shown that WT MC1R, but not several major RHC alleles, might prevent proteasomal degradation of PTEN[35], suggesting the possibility of a differential capability to activate AKT signalling. Both the ERKs[36–38] and AKT[39–41] play roles in DNA repair. Taken together, these observations suggest that variant *MC1R* with disrupted cAMP signalling might still be able to activate DNA damage responses. To test this hypothesis, we assessed MC1R-dependent protection against oxidative DNA damage in human melanoma cells (HMCs) and epidermal melanocytes of defined *MC1R* genotype. Given the relevance of oxidatively-generated DNA damage in the presence of pheomelanic pigmentation associated with *MC1R* variants[6], we focused on major oxidative lesions, namely 8-oxo-7,8-dihydro-2'-deoxyguanine (8-oxodG) and single or double strand breaks (SSBs or DSBs)[42]. We show the occurrence of cAMP-independent DNA repair mechanisms downstream of variant MC1R. We also show that variant MC1R activates AKT to promote DNA repair.

RESULTS

Induction of DNA repair downstream of variant MC1R

To investigate the effect of *MC1R* genotype on susceptibility to oxidative DNA damage, we first used two HMC lines, HBL and A375. HBL cells are WT for *MC1R*, *NRAS* and *BRAF*, whereas A375 cells carry the V600E *BRAF* mutation and are homozygous for the R151C *MC1R* variant (Supplementary Table S1). To mimic transient oxidative stress, cells were pulsed with tert-butyl hydroperoxide (Luperox) ($1.5x10^{-4}$ M, 30 min), used as a stable form of H_2O_2[43]. This treatment increased comparably ROS levels without significant effects on cell viability not only in A375 and HBL cells, but also in two other HMC lines (SKMEL28 and C8161) and Hermes human melanocytes (Supplementary Figures S1a, S1b). The oxidative challenge was performed with or without pretreatment (36 h) with the stable αMSH analogue NDP-MSH, the adenylyl cyclase (AC) activator forskolin (FSK) or the cell-permeable cAMP precursor dibutyryl-cAMP (dbcAMP). Then, Luperox-treated cells were stained for 8-oxodG, a major product of UVR-induced oxidative DNA damage. For *MC1R*-WT HBL cells, Luperox strongly increased 8-oxodG staining. This increase was abolished by the non-selective antioxidant ebselen[44] or by pretreatment with NDP-MSH, FSK or dbcAMP (Figure 1a and Supplementary Figure S1c). These treatments dramatically increased intracellular cAMP levels (Figure 1b). Furthermore, the AC inhibitor 2′,5′-dideoxyadenosine (DDA) blocked NDP-MSH or FSK-dependent cAMP production and decreased markedly their

protective effect (Figures 1a and 1b). Therefore, in WT *MC1R* HBL cells, the cAMP pathway contributed most of the MC1R-dependent reduction of ROS-induced oxidative DNA damage as assessed by 8-oxodG staining, in agreement with reports by others[29–31].

Pretreatment of *MC1R*-variant A375 cells with NDP-MSH also decreased 8-oxodG levels compared with treatment with Luperox alone (Figure 1c), but NDP-MSH failed to activate cAMP signalling as demonstrated by lack of stimulation of cAMP levels or *MITF* gene expression (Figure 1d and 1f). Thus, in A375 cells homozygous for the R151C allele, MC1R activation triggered a significant protective response most likely in a cAMP-independent manner. Interestingly, pretreatment of A375 HMCs with dbcAMP, but not FSK, achieved a strong increase in intracellular cAMP and had a strong protective effect against ROS-induced DNA oxidative damage (Figures 1c, 1d). This showed that the cAMP-activated pathway(s) responsible for protection against DNA oxidative insults remained operative in A375 cells.

Next, we analyzed variant MC1R-dependent protection against peroxide-generated DNA strand breaks (SBs). Exposure of cells to ROS such as peroxyl radicals increases SBs[45]. Whereas low micromolar peroxide concentrations mostly induce SSBs, relatively high concentrations such as those employed here also induce significant numbers of DSBs[46]. ROS-induced DSBs rapidly result in phosphorylation of histone H2AX**.** Phosphorylated H2AX (γH2AX) attracts repair factors to DSB sites, forming foci enriched in repair proteins[47]. In the same experimental conditions as for determination of 8-oxodG, Luperox treatment augmented γH2AX staining in HBL and A375 cells (Figures 2a, 2b). Preincubation with NDP-MSH prevented the increase in γH2AX staining in both cell lines, suggesting reduction of DSBs. The possibility that γH2AX foci, which are poorly induced by SSBs, might arise by conversion of such lesions to DSBs on passage of a replication fork in proliferating cells appeared unlikely, since a clear majority of cells exhibited extensive and similar staining (Figures 2c and 2d). Moreover, incubation with NDP-MSH, which reduced strongly γH2AX staining, had little effect on cell cycle progression (Figure 2e).

On the other hand, pretreatment of HBL cells with either FSK or dbcAMP also decreased the γH2AX signal. Conversely, only dbcAMP afforded protection to A375 cells (Supplementary Figure S2) but FSK was ineffective, in keeping with its previously observed inability to decrease peroxide-induced 8-oxodG or to activate significantly cAMP synthesis in these cells.

We wished to confirm MC1R-mediated reduction of DNA SBs in MC1R-variant A375 cells. To this end, we assessed oxidative DNA fragmentation using the alkaline comet assay. In HBL and A375 cells, NDP-MSH reduced Luperox-induced DNA SBs

(Figures 2f, 2g and Supplementary Table 2). As for γH2AX staining, preincubation with FSK decreased Luperox-generated SBs in HBL cells but not in A375 HMCs, whereas dbcAMP reduced SBs in both cell types. These data confirmed the involvement of cAMP- independent pathways in protection against oxidative DNA damage downstream of variant MC1R. Of note, the DNA damage repair response triggered by cAMP remained operative in these cell lines, as it could be evoked by dbcAMP.

To confirm the novel finding of cAMP-independent protective mechanisms downstream of variant MC1R, we analyzed three other melanocytic cell lines, SKMEL28 and C8161 HMCs and Hermes melanocytes. C8161 are heterozygotes for R151C *MC1R* and bear the V600E *BRAF* mutation (Supplementary Table S1). SKMEL28 cells carry the V600E *BRAF* mutation and the T167A *PTEN* mutation (Supplementary Figure S3a) causing partial loss-of-function with retention of significant phosphatase activity[48]. SKMEL28 cells are compound heterozygotes for *MC1R*, bearing the I155T R variant[49] and another variant allele, S83P, of unknown functional behaviour. We cloned the S83P variant for functional analysis. Upon stimulation with NDP-MSH, S83P MC1R expressed in HEK293T cells did not activate the cAMP pathway but retained full capacity to activate the ERKs (Supplementary Figure S3b-d). Therefore, S83P behaved as a strong R allele. We also found that Hermes melanocytes were *MC1R* heterozygotes carrying a natural variant allele coding for a $C275^{STOP}$ truncated protein. Cys275 is located within the 3rd extracellular loop of the receptor, and accordingly $C275^{STOP}$ lacks the complete 7th transmembrane fragment and cytosolic extension of the native receptor. We did not analyze this variant for function since our previous studies have shown that removal of the same regions in an artificial $C273^{STOP}$ mutant, or the C-terminal cytosolic extension in $Y298^{STOP}$ lead to complete loss of signalling to the cAMP pathway[50,51]. Treatment of SKMEL28, C8161 or Hermes cells with NDP-MSH did not increase cAMP levels (Supplementary Figure S4a). On the other hand, NDP-MSH transiently stimulated the ERKs in Hermes melanocytes (Supplementary Figure S4b).

Preincubation of C8161, SKMEL28 or Hermes cells with NDP-MSH comparably decreased the steady state levels of DNA SBs generated by Luperox (Supplementary Figure S5a). This suggested that the cAMP-independent protection against oxidative DNA fragmentation afforded by NDP-MSH in A375 cells was not an artefact of this cell type but was rather a general behaviour of MC1R-variant melanocytic cells. To further establish the ability of variant MC1R to protect against oxidative DNA damage, we transfected HEK293T cells with Flag epitope-labeled WT or R151C MC1R. At comparable expression levels, NDP-MSH elicited a similar protective response against

Luperox-induced DNA fragmentation, as estimated by comet assays (Supplementary Figure S5b).

The experiments described thus far were performed using a relatively long oxidative challenge (30 min) and a prolonged preincubation with NDP-MSH (36 h) that may allow for the induction of antioxidant enzymes. Therefore, the protective effect of MC1R activation could result from a combination of augmented clearance of oxidative lesions and decreased oxidative damage due to improved antioxidant defenses. To assess the relative contribution of these non-mutually exclusive mechanisms, we investigated the extent and kinetics of induction of antioxidant enzymes downstream of WT or variant MC1R. HBL or A375 cells were treated with NDP-MSH, and the expression of *catalase* (*CAT*), *superoxide dismutase* (*SOD1*) and *glutathione peroxidase* (*GPx1*) genes was assessed. For HBL cells, NDP-MSH caused a time-dependent induction of *CAT*, a faster stimulation of *SOD1* and a weaker increase in *GPx1* expression. These stimulatory effects were abolished by DDA-mediated inhibition of AC (Figure 3a). Moreover, upregulation of intracellular cAMP levels by FSK or dbcAMP also increased expression of *CAT*, *SOD1* and *GPx1* in HBL cells (Supplementary Figure S6a). These data were consistent with reports of cAMP-dependent upregulation of antioxidant enzymes downstream of WT MC1R[29–31]. Concerning A375 cells, NDP-MSH (Figure 3b) or FSK (Supplementary Figure S6b) had little effect on *CAT* expression and did not increase *GPx1* mRNA, whereas dbcAMP significantly stimulated *SOD* and *CAT* expression (Supplementary Figure S6b). Surprisingly, in A375 cells NDP-MSH and FSK upregulated potently and transiently *SOD1* expression, suggesting that in these cells signalling mechanisms different from the cAMP pathway could be responsible for *SOD1* upregulation downstream of MC1R.

We analyzed catalase and SOD1 protein levels upon MC1R stimulation with NDP-MSH for up to 48 h. We observed a significant induction of catalase in agonist-treated HBL cells, but A375 cells were unresponsive (Figure 3c). Expression of SOD1 did not change significantly in either cell type (Figure 3d). To find out whether upregulation of catalase led to a decreased ROS burden, we measured total ROS levels in NDP-MSH-treated cells. We found a trend towards lower ROS levels in NDP-MSH-stimulated cells that did not reach statistical significance (Figure 3e). Therefore, WT MC1R HMCs may cope with oxidative stress by induction of antioxidant enzymes in response to activation of the cAMP pathway. However, this effect would be small, and absent in *MC1R* variant HMCs. Accordingly, the protection against DNA damage in A375 cells treated with NDP-MSH most likely resulted from enhanced DNA repair.

To confirm activation of DNA repair pathways downstream of variant MC1R, we compared the rate of clearance of oxidative DNA lesions in control cells or cells

pretreated with NDP-MSH for 36 h. For this purpose, HBL and A375 HMCs kept on ice were challenged with Luperox for a shorter time (10 min), then quickly washed and incubated at 37ºC to follow the kinetics of 8-oxodG removal and comet tail clearance. In the absence of NDP-MSH, the intensity of 8-oxodG staining and the comet tail moments stayed constant for up to 15 min after removal of the oxidizing agent in HBL cells or even increased slightly in A375 cells (Figure 4). Conversely, NDP-MSH-treated cells showed a progressive clearance of 8-oxodG and a reduction of the comet tail moments, already noticeable after a 5 min recovery, thus confirming active DNA repair.

Involvement of AKT signalling in the protective effect of variant MC1R

We aimed at identifying MC1R-triggered, cAMP-independent signalling pathway(s) responsible for the protective effects of NDP-MSH in *MC1R*-variant cells. We showed previously that NDP-MSH triggers ERK activation by cAMP-independent transactivation of cKIT[14,33]. Thus, we assessed the effect of the ERK pathway inhibitor PD98059 on MC1R-induced DNA repair. In HBL cells, PD98059 inhibited effectively basal and NDP-MSH-induced ERK activity and decreased, but did not abolish, protection against oxidative DNA fragmentation afforded by NDP-MSH. Indeed, Luperox-challenged HBL cells pre-stimulated with NDP-MSH in the presence of PD98059 showed significant reductions of comet tail moments (Figure 5a). For A375 cells, NDP-MSH decreased comparably oxidative DNA SBs, in the presence or absence of PD98059 (Figure 5b), despite nearly complete ERK inhibition. We obtained similar results for SKMEL28 cells (Supplementary Figure S7). These observations ruled out ERK activation as responsible for protection against oxidative DNA fragmentation downstream of variant *MC1R*.

Next, we challenged HBL and A375 cells with NDP-MSH and compared the activatory AKT phosphorylation. NDP-MSH did not augment AKT phosphorylation in WT *MC1R* HBL cells but activated AKT in A375 cells (Figure 6a). We observed a comparable activation of AKT in NDP-MSH-treated SKMEL28, C8161 and Hermes cells, with peak levels at 60-90 min (Supplementary Figure S8a). Therefore, variant MC1R activated AKT efficiently, but AKT activation downstream of MC1R was undetectable in cells expressing WT MC1R. This suggested an inverse relationship between AKT activation and the cAMP pathway. Since high cAMP levels inhibit AKT in B16 mouse melanoma cells[52], we reasoned that a similar inhibition might occur in human cells. To test this possibility, we blocked AC activation with DDA in HBL cells, and we increased cAMP levels in A375 cells with dbcAMP. Then, we challenged cells with NDP-MSH and compared pAKT levels. DDA allowed activation of AKT downstream of MC1R in HBL cells, whereas elevation of cAMP in A375 melanoma

cells abolished AKT phosphorylation (Figure 6b). Similar results were obtained for SKMEL28, C8161 and Hermes cells (Supplementary Figure 8b).

Since AKT was activated downstream of variant MC1R, we checked its involvement in MC1R-dependent reduction of oxidative DNA damage. We blocked the AKT pathway with pharmacological inhibitors and analyzed comet tail moments in Luperox-pulsed cells. We used LY94002 and MK-2206 to block PI3K and AKT activation, respectively[53]. This treatment prevented AKT activation and abolished the protective action of NDP-MSH in A375 but not in HBL cells (Figures 6c, 6d and Supplementary Figure S9). Moreover, this treatment also blocked protection in C8161, SKMEL28 and Hermes cells (Supplementary Figure S8c-e). To confirm a protective effect of AKT signalling in MC1R-variant melanoma cells, the oxidative challenge was performed in cells pretreated with SC79, an agonist of the AKT pathway which binds to AKT to induce a conformation favorable for phosphorylation by upstream activatory kinases[54]. SC79 had no effect on tail moments in HBL cells, consistent with its inability to increase pAKT levels in these cells (Figure 6c). Conversely, SC79 activated AKT efficiently in A375 cells (Figure 6d) and reduced Luperox-induced comet tail moments. Again, we observed a similar behaviour in other melanocytic cells (Supplementary Figure S8c-e). Therefore, the PI3K/AKT pathway was involved in NDP-MSH-induced clearance of DNA SBs downstream of variant MC1R.

DISCUSSION

WT *MC1R* protects against melanomagenesis by a combination of pigmentation-dependent and independent mechanisms[1]. The main external etiologic factor for melanoma is solar UVR, which causes direct DNA damage through its UVB component, or ROS-induced lesions through less energetic UVA radiation[3,4,55] resulting in high mutational rates. The pigmentation-dependent component of *MC1R* protective action is accounted for by a switch from basal pheomelanogenesis to eumelanogenesis. Eumelanin is a photoprotective pigment owing to its absorption properties in the UVR spectrum and its free radical scavenging properties[56]. Conversely, pheomelanin is a photosensitizer promoting ROS production upon exposure to UVR[5,57–59], that can reduce the intracellular antioxidant pool even in the absence of UVR[60]. Accordingly, pheomelanins promote melanomagenesis in mice carrying a conditional *BRAF*-mutant allele[6]. Concerning non-pigmentary actions, WT MC1R signalling activates antioxidant enzymes[28,30] and DNA repair pathways[61,62]. Owing to this combination of pigment-dependent and -independent effects, the

mutation load in WT *MC1R* melanomas is lower compared with *MC1R*-variant melanomas[63–65].

MC1R triggers several signalling pathways, and most *MC1R* alleles associated with higher melanoma risk are not loss-of-function variants *sensu stricto,* since they activate the ERKs with an efficiency comparable with WT, despite impaired cAMP signalling[1,14,33,34]. The pheomelanogenesis/eumelanogenesis switch depends upon activation of the cAMP pathway [66–69]. Therefore, inefficient cAMP signalling accounts for the pigmentary component of the association of *MC1R* variants and melanoma risk. Moreover, cAMP signalling stimulates non-pigmentary protective responses, including activation of base and nucleotide excision repair (BER and NER)[29–31,70]. However, ERK and AKT signalling play important roles in the activation of cell cycle checkpoints in response to DNA damage and in the induction of DNA repair mechanisms[39,71]. Therefore, *MC1R* alleles unable to promote cAMP-dependent eumelanogenesis might still be able to trigger cAMP-independent non-pigmentary responses. Thus, we compared the response of HMCs of defined *MC1R* genotype to oxidative challenges mimicking UVA-induced oxidative stress.

We found that NDP-MSH reduced significantly oxidative DNA damage in human melanoma cells of WT or variant *MC1R* genotype, as shown by decreased steady-state levels of 8-oxodG, γH2AX foci and DNA SBs. In HBL cells expressing WT MC1R, this protective effect may be partially accounted for by increased antioxidant defenses, since a significant induction of catalase by NDP-MSH was detected. However, in A375 cells expressing the hypomorphic R151C MC1R variant, this protective effect occurred without induction of antioxidant enzymes, pointing to activation of DNA repair, which was confirmed by kinetic analysis of clearance of oxidative DNA lesions after short Luperox challenges. Therefore, our data showed that variant *MC1R* can activate DNA repair.

Since *MC1R*-variant melanocytic cells used in this study failed to activate the cAMP pathway downstream of MC1R, we looked for the signalling pathways involved in their pigment-independent protective action. In MC1R-variant cells, NDP-MSH decreased comparably Luperox-induced DNA fragmentation in the absence or presence of the MEK inhibitor PD98059 (Figure 5), thus ruling out involvement of ERK signalling in the DNA protective effect. On the other hand, NDP-MSH significantly activated AKT in cells of variant *MC1R* genetic background. AKT is directly involved in DNA repair processes[39,71], promoting non-homologous end joining (NHEJ)-mediated repair of DSBs after irradiation of cancer cells[72], and inducing the BER of oxidized bases through activation of nuclear factor erythroid 2-related factor 2 (Nrf2) and subsequent upregulation of 8-oxoguanine glycosylase 1 (OGG1)[73,74]. This mechanism

has been recently shown to account for the protection against UVB-induced damage afforded by melatonin treatment of cultured human melanocytes[75]. In keeping with the protective role of AKT in other cell types, the AKT activator SC79 decreased the number of DNA SBs in Luperox-treated *MC1R*-variant HMCs. Moreover, blocking AKT signalling with LY94002 and MK-2206 abolished variant *MC1R*-dependent activation of DNA repair. Notably, in melanoma cells WT for MC1R, neither NDP-MSH nor SC79 activated AKT. Conversely, blocking cAMP production in these cells with DDA rescued AKT activation downstream of MC1R. On the other hand, pharmacological elevation of cAMP levels in *MC1R* variant HMCs also blocked AKT activation downstream of MC1R (Figure 6). Therefore, cAMP inhibited AKT signalling in HMCs, as previously shown for mouse melanoma cells[52,69]. Consistent with lack of AKT activation downstream of WT MC1R, induction of protective responses by NDP-MSH was unaffected by LY94002 and MK-2206. Conversely, these responses were blocked by DDA and mimicked by FSK or dbcAMP, confirming their dependence on cAMP. However, our data do not exclude the possible occurrence of ERK-dependent SB repair in MC1R-WT cells. Accordingly, our results suggest a model whereby MC1R activation promotes protection against oxidative DNA damage at least by two mechanisms, one of them dependent on cAMP and operative in MC1R-WT cells, whereas the other would depend on AKT and would be restricted to *MC1R*-variant cells (Figure 7).

The pathway linking variant MC1R to AKT activation remains unclear. The level of active, phospho-AKT reflects the balance between the opposing actions of activatory kinases working in a phosphatidylinositol triphosphate (PIP_3)-PI3K-dependent manner on one hand, and dephosphorylation by PP2A or PHLPP phosphatases on the other[76]. In turn, PI3K-PIP_3 signaling is activated downstream of RTKs or GPCRs and is terminated by PTEN. In human melanocytes, MC1R activates the cKIT RTK[33], but treatment of A375 cells with the cKIT inhibitors AG1478 or dasatinib did not block AKT activation by NDP-MSH (data not shown). In turn, PI3K activation by GPCRs most often relies on G protein activation via release of βγ dimers from αβγ heterotrimers[77]. However, MC1R variants do not stimulate efficiently cAMP synthesis indicating that they do not achieve significant levels of G protein activation. Accordingly, AKT activation by variant MC1R might result from interference with an inhibitory phosphatase, rather than activation of upstream kinase(s). This possibility is consistent with the slow kinetics of AKT activation by NDP-MSH in MC1R-variant cells. Notably, in MSH-treated UV-irradiated melanocytes, WT MC1R recruits PTEN in an interaction that prevents PTEN ubiquitination by WWP2, thereby protecting the phosphatase from proteasomal degradation[35]. The resulting PTEN stabilization partially downregulates AKT signaling. Conversely, MC1R variants such as R151C interact poorly with PTEN,

allowing for PTEN degradation and higher AKT activity. On the other hand, cAMP can activate PP2A, leading to inactivation of AKT[78–80]. Accordingly, a differential regulation of the levels or activity of phosphatases might underlie the different effect of WT and variant MC1R on AKT. This possibility is currently under study.

Oxidative injury to guanine and SSBs are usually repaired by BER, whereas DSBs are cleared by homologous recombination (HR) or NHEJ[39,65]. Variant MC1R accelerates clearance of 8-oxodG, the DSB marker γH2AX and comet tails, and therefore it might stimulate BER as well as HR or NHEJ. Activation of BER downstream of WT MC1R has been demonstrated[29], but the MC1R-regulated genes/proteins responsible for this protective effect remain largely unknown. Notably, two key components of BER, OGG1 and apurinic apyrimidinic endonuclease 1 (APE-1/Ref-1) are induced in MSH-treated melanocytes[29], and the pathways accounting for these effects remain uncharacterized. The involvement of AKT is likely, since AKT activates APE-1/Ref-1 in other cell types[81] and also regulates OGG1 activity, although in this case both inhibition and activation were reported, suggesting cell-type or context-dependent effects[73,74,82]. The latter activation occurs via AKT-mediated induction of the nuclear factor Nrf2 in response to oxidative stress[73–75].

In summary, here we showed that AKT was activated downstream of variant MC1R in human melanocytic cells. This activation was blunted downstream of the WT receptor due to a suppressive effect of cAMP. We also showed that variant MC1R accelerated the AKT-dependent clearance of 8-oxodG and DNA SBs, implying that it activated BER and recombinational repair. It remains to be seen how these observations can be reconciled with higher mutation loads in melanomas of variant *MC1R* genetic background compared with *MC1R*-WT melanomas[63,64]. In this respect, several possibilities can be considered. Variant MC1R may not activate NER-mediated clearance of UVB-produced lesions such as cyclobutene pyrimidine dimers as effectively as WT. Moreover, the precise cAMP-dependent DNA repair pathways triggered by WT MC1R may not be the same as the AKT-dependent pathways activated by variant MC1R. AKT plays opposite roles in the two major types of NER by promoting transcription-coupled NER while inhibiting global genome NER[39]. Concerning repair of DSBs, AKT was shown to inhibit HR while activating NHEJ[39,83]. Importantly, NHEJ may be particularly important for DSB clearance in UVR-irradiated melanocytes, since UVR induces G1 cell cycle arrest[84] and HR is restricted to the S and G2 phases[85]. The possibility of a differential engagement of DSB repair pathways by WT and variant MC1R is currently under study. In any case, our demonstration of AKT-dependent DNA repair downstream of variant MC1R may be important for the

design of rational melanoma prevention treatments such as application of topical agents increasing cAMP levels in sun-exposed skin.

METHODS

Cell culture

Cell culture reagents were from Gibco (Gaithersburg, MD) or Gentaur (Kampenhout, Belgium). Melanoma cells and HEK293T cells were grown in DMEM with 10% fetal bovine serum (FBS). Hermes melanocytes were cultured in Melanocyte Medium-2 with 5% FBS and 10% Melanocyte Growth Supplement-PMA-free. Serum and supplements were removed 1 day before, and during each experiment.

Expression constructs and transfection

Flag-tagged WT and variant MC1R has been described[86]. S83P MC1R was obtained by site-directed mutagenesis with the QuikChange XL Site-Directed Mutagenesis kit (Agilent, Santa Clara, CA) using Flag-WT-MC1R as template. HEK293T cells were transfected with 0.15 or 0.3 µg of plasmid DNA/well for 24 or 12-well plates, respectively, using Lipofectamine 2000 (Invitrogen) and Opti-MEM (Gibco).

Analysis of *MC1R* and *PTEN* mutation status

MC1R and *PTEN* ORFs were amplified from cDNA obtained using SuperScript™ III First-Strand Synthesis System (Invitrogen) and sequenced from two different PCR reactions to confirm each mutation. See Supplementary Table 3 for details on amplification procedures.

Immunoblotting

Western blotting was performed as described[87] using antibodies summarized in Supplementary Table 4.

Functional assays

cAMP was determined using a commercial immunoassay from Arbor Assays (Eisenhower Place, Michigan, USA)[88].

Immunofluorescence, confocal microscopy and image quantification

For 8-oxodG staining, HBL and A375 cells fixed with methanol followed by acetone at -20° C were treated with 0.05N HCl (5 min, 4º C) and 100 µg/ml RNAse (1 h, 37° C). DNA was denatured *in situ* with 0.15 N NaOH in 70% EtOH. Cells were incubated in 5 µg/ml proteinase K for 10 min at 37° C, blocked with 5% goat serum and incubated with anti-8-oxodG (Trevigen, Gaithersburg, MD, USA), followed by an Alexa 488-conjugated secondary antibody (Molecular Probes, Invitrogen), and with DAPI (10 µg/ml, Invitrogen Life Technologies).

For γ-H2AX staining, HBL and A375 cells fixed with 4% *p*-formaldehyde, were permeabilized with 0.5% Triton-X 100 (v/v) and blocked with 5% BSA. Cells were

labeled with anti-γH2A.X (phospho-S139) monoclonal antibody (Abcam, Cambridge, UK), followed by an Alexa 488-conjugated secondary antibody. Images were analyzed using Qwin Software (Leica Microsystems Ltd., Barcelona, Spain).

Intracellular ROS assay

ROS levels were assessed with 2′7′dichlorodihydrofluorescein diacetate (Molecular Probes). Fluorescence was measured at 492 nm excitation and 517 nm emission and normalized for cell numbers with crystal violet.

Comet assay

The Alkaline Comet Assay was performed per the manufacturer's protocol (Trevigen). DNA was unwound by treatment in alkaline electrophoresis solution, pH>13 (200 mM NaOH, 1 mM EDTA) for 20 min, and stained with Midori Green advanced (Nippon genetics Europe, Düren, Germany). Images were taken using a Leica fluorescence microscope. Quantitative analysis of tail moments of at least 100 randomly selected comets per sample was performed using CASPLAB software (http://www.casp.of.pl).

Gene expression analysis by real-time PCR

Cells were serum-deprived at least 12 h before RNA extraction with RNeasy (QIAGEN, Hilden, Germany). One µg of RNA was reverse-transcribed using SuperScript® III. RT-PCR was performed using the Power SYBR Green PCR Master Mix (Applied Biosystem) on ABI 7500 Fast Real Time PCR System. β-actin was used as endogenous normalizer. See Supplementary Table 5 for primers sequences.

Statistical analysis

Experiments were performed with at least three biological replicates. The sample size was chosen using GRANMO (https://www.imim.es/ofertadeserveis/software-public/granmo/index.html) and is indicated in figure legends. No samples were excluded from any analyses. Subpopulations of cells were randomly assigned to treatments. Blind analysis was not performed in this study. Statistical significance was assessed using GraphPad Software (San Diego California, USA). Data met the assumptions of the test used. We used D'Angostino-Pearson omnibus normality test for Gaussian distribution. Unpaired two-tailed Student's t-test and one-way ANOVA with Tukey post-test for multiple comparisons were performed when variance among groups was not statistically different. Otherwise, we used one-way Kruskal-Wallis test. Results are expressed as mean±SEM. p values were calculated using two-sided tests.

ACKNOWLEDGEMENTS

Supported by grants SAF2015-67092-R from MINECO (Spain) and FEDER (European Community) and 19875/GERM/15 from Fundación Seneca, Comunidad Autónoma de

la Región de Murcia (CARM). M Castejón holds a pre-doctoral fellowship from the Fundación Seneca. Cecilia Herraiz was a Juan de la Cierva-Incorporación fellow of MINECO. We thank Prof G Ghanem, from the Free University of Brussels for gift of human melanoma cell lines and Prof Neptuno Rodríguez (University of Murcia) for Hermes melanocytes. We also thank Prof. J.L. Castejón for help with the statistical analysis of data, Dr. M. Abrisqueta for assistance in cell cycle analysis and Dr. A. López-Contreras for suggestions and critical reading of the manuscript.

CONFLICT OF INTEREST

The authors declared no conflict of interest.

REFERENCES

1 Garcia-Borron JC, Abdel-Malek Z, Jimenez-Cervantes C. MC1R, the cAMP pathway, and the response to solar UV: extending the horizon beyond pigmentation. *Pigment Cell Melanoma Res* 2014; **27**: 699–720.

2 Merlino G, Herlyn M, Fisher DE, Bastian BC, Flaherty KT, Davies MA *et al.* The state of melanoma: challenges and opportunities. *Pigment Cell Melanoma Res* 2016; **29**: 404–16.

3 Krauthammer M, Kong Y, Ha BH, Evans P, Bacchiocchi A, McCusker JP *et al.* Exome sequencing identifies recurrent somatic RAC1 mutations in melanoma. *Nat Genet* 2012; **44**: 1006–1014.

4 Hodis E, Watson IR, Kryukov G V, Arold ST, Imielinski M, Theurillat JP *et al.* A landscape of driver mutations in melanoma. *Cell* 2012; **150**: 251–263.

5 Napolitano A, Panzella L, Monfrecola G, d'Ischia M. Pheomelanin-induced oxidative stress: bright and dark chemistry bridging red hair phenotype and melanoma. *Pigment Cell Melanoma Res* 2014; **27**: 721–733.

6 Mitra D, Luo X, Morgan A, Wang J, Hoang MP, Lo J *et al.* An ultraviolet-radiation-independent pathway to melanoma carcinogenesis in the red hair/fair skin background. *Nature* 2012; **491**: 449–453.

7 Box NF, Wyeth JR, O'Gorman LE, Martin NG, Sturm RA. Characterization of melanocyte stimulating hormone receptor variant alleles in twins with red hair. *Hum Mol Genet* 1997; **6**: 1891–7.

8 Smith R, Healy E, Siddiqui S, Flanagan N, Steijlen PM, Rosdahl I *et al.* Melanocortin 1 Receptor Variants in an Irish Population. *J Invest Dermatol* 1998; **111**: 119–122.

9 Valverde P, Healy E, Jackson I, Rees JL, Thody a J. Variants of the melanocyte-stimulating hormone receptor gene are associated with red hair and

fair skin in humans. *Nat Genet* 1995; **11**: 328–330.

10 Davies JR, Randerson-Moor J, Kukalizch K, Harland M, Kumar R, Madhusudan S *et al.* Inherited variants in the MC1R gene and survival from cutaneous melanoma: a BioGenoMEL study. *Pigment Cell Melanoma Res* 2012; **25**: 384–394.

11 Dessinioti C, Antoniou C, Katsambas A, Stratigos AJ. Melanocortin 1 receptor variants: functional role and pigmentary associations. *Photochem Photobiol*; **87**: 978–87.

12 Scherer D, Kumar R. Genetics of pigmentation in skin cancer--a review. *Mutat Res* 2010; **705**: 141–153.

13 Frandberg PA, Doufexis M, Kapas S, Chhajlani V. Human pigmentation phenotype: a point mutation generates nonfunctional MSH receptor. *Biochem Biophys Res Commun* 1998; **245**: 490–492.

14 Herraiz C, Jimenez-Cervantes C, Zanna P, Garcia-Borron JC. Melanocortin 1 receptor mutations impact differentially on signalling to the cAMP and the ERK mitogen-activated protein kinase pathways. *FEBS Lett* 2009; **583**: 3269–3274.

15 Nakayama K, Soemantri A, Jin F, Dashnyam B, Ohtsuka R, Duanchang P *et al.* Identification of novel functional variants of the melanocortin 1 receptor gene originated from Asians. *Hum Genet* 2006; **119**: 322–330.

16 Newton RA, Smit SE, Barnes CC, Pedley J, Parsons PG, Sturm RA. Activation of the cAMP pathway by variant human MC1R alleles expressed in HEK and in melanoma cells. *Peptides* 2005; **26**: 1818–1824.

17 Ringholm A, Klovins J, Rudzish R, Phillips S, Rees JL, Schiöth HB. Pharmacological characterization of loss of function mutations of the human melanocortin 1 receptor that are associated with red hair. *J Invest Dermatol* 2004; **123**: 917–923.

18 Roberts DW, Newton RA, Leonard JH, Sturm RA. Melanocytes expressing MC1R polymorphisms associated with red hair color have altered MSH-ligand activated pigmentary responses in coculture with keratinocytes. *J Cell Physiol* 2008; **215**: 344–55.

19 Schiöth HB, Phillips SR, Rudzish R, Birch-Machin M a, Wikberg JE, Rees JL. Loss of function mutations of the human melanocortin 1 receptor are common and are associated with red hair. *Biochem Biophys Res Commun* 1999; **260**: 488–491.

20 Scott MC, Wakamatsu K, Ito S, Kadekaro AL, Kobayashi N, Groden J *et al.* Human melanocortin 1 receptor variants, receptor function and melanocyte response to UV radiation. *J Cell Sci* 2002; **115**: 2349–2355.

21 Sanchez-Laorden BL, Sanchez-Mas J, Martinez-Alonso E, Martinez-Menarguez JA, Garcia-Borron JC, Jimenez-Cervantes C. Dimerization of the human melanocortin 1 receptor: functional consequences and dominant-negative effects. *J Invest Dermatol* 2006; **126**: 172–181.

22 Garcia-Borron JC, Olivares C. Melanocortin 1 receptor and skin pathophysiology: beyond colour, much more than meets the eye. *Exp Dermatol* 2014; **23**: 387–388.

23 Fajuyigbe D, Young AR. The impact of skin colour on human photobiological responses. *Pigment Cell Melanoma Res* 2016; **29**: 607–618.

24 Bastiaens MT, ter Huurne J a, Kielich C, Gruis N a, Westendorp RG, Vermeer BJ *et al.* Melanocortin-1 receptor gene variants determine the risk of nonmelanoma skin cancer independently of fair skin and red hair. *Am J Hum Genet* 2001; **68**: 884–894.

25 Gerstenblith MR, Goldstein AM, Fargnoli MC, Peris K, Landi MT. Comprehensive evaluation of allele frequency differences of MC1R variants across populations. *Hum Mutat* 2007; **28**: 495–505.

26 Bohm M, Wolff I, Scholzen TE, Robinson SJ, Healy E, Luger TA *et al.* alpha-Melanocyte-stimulating hormone protects from ultraviolet radiation-induced apoptosis and DNA damage. *J Biol Chem* 2005; **280**: 5795–5802.

27 Kadekaro AL, Kavanagh R, Kanto H, Terzieva S, Hauser J, Kobayashi N *et al.* alpha-Melanocortin and endothelin-1 activate antiapoptotic pathways and reduce DNA damage in human melanocytes. *Cancer Res* 2005; **65**: 4292–4299.

28 Kadekaro AL, Leachman S, Kavanagh RJ, Swope V, Cassidy P, Supp D *et al.* Melanocortin 1 receptor genotype: an important determinant of the damage response of melanocytes to ultraviolet radiation. *FASEB J* 2010; **24**: 3850–3860.

29 Kadekaro AL, Chen J, Yang J, Chen S, Jameson J, Swope VB *et al.* Alpha-Melanocyte-Stimulating Hormone Suppresses Oxidative Stress through a p53-Mediated Signaling Pathway in Human Melanocytes. *Mol Cancer Res* 2012; **10**: 778–786.

30 Maresca V, Flori E, Bellei B, Aspite N, Kovacs D, Picardo M. MC1R stimulation by alpha-MSH induces catalase and promotes its re-distribution to the cell periphery and dendrites. *Pigment Cell Melanoma Res* 2010; **23**: 263–75.

31 Song X, Mosby N, Yang J, Xu A, Abdel-Malek Z, Kadekaro AL. alpha-MSH activates immediate defense responses to UV-induced oxidative stress in human melanocytes. *Pigment Cell Melanoma Res* 2009; **22**: 809–18.

32 Herraiz C, Garcia-Borron JC, Jiménez-Cervantes C, Olivares C. MC1R signaling. Intracellular partners and pathophysiological implications. *Biochim*

Biophys Acta - Mol Basis Dis 2017. doi:10.1016/j.bbadis.2017.02.027.

33 Herraiz C, Journe F, Abdel-Malek Z, Ghanem G, Jimenez-Cervantes C, Garcia-Borron JC. Signaling from the human melanocortin 1 receptor to ERK1 and ERK2 mitogen-activated protein kinases involves transactivation of cKIT. *Mol Endocrinol* 2011; **25**: 138–156.

34 Herraiz C, Journe F, Ghanem G, Jimenez-Cervantes C, Garcia-Borron JC. Functional status and relationships of melanocortin 1 receptor signaling to the cAMP and extracellular signal-regulated protein kinases 1 and 2 pathways in human melanoma cells. *Int J Biochem Cell Biol* 2012; **44**: 2244–2252.

35 Cao J, Wan L, Hacker E, Dai X, Lenna S, Jimenez-Cervantes C *et al.* MC1R is a potent regulator of PTEN after UV exposure in melanocytes. *Mol Cell* 2013; **51**: 409–422.

36 Cohen-Armon M. PARP-1 activation in the ERK signaling pathway. *Trends Pharmacol Sci* 2007; **28**: 556–60.

37 Wei F, Yan J, Tang D. Extracellular signal-regulated kinases modulate DNA damage response - a contributing factor to using MEK inhibitors in cancer therapy. *Curr Med Chem* 2011; **18**: 5476–82.

38 Hawkins AJ, Golding SE, Khalil A, Valerie K. DNA double-strand break - induced pro-survival signaling. *Radiother Oncol* 2011; **101**: 13–7.

39 Liu Q, Turner KM, Alfred Yung WK, Chen K, Zhang W. Role of AKT signaling in DNA repair and clinical response to cancer therapy. *Neuro Oncol* 2014; **16**: 1313–1323.

40 Toulany M, Rodemann HP. Phosphatidylinositol 3-kinase/Akt signaling as a key mediator of tumor cell responsiveness to radiation. *Semin Cancer Biol* 2015; **35**: 180–190.

41 Singh P, Dar MS, Dar MJ. p110α and p110β isoforms of PI3K signaling: are they two sides of the same coin? *FEBS Lett* 2016; **590**: 3071–3082.

42 Cadet J, Douki T, Ravanat J-L. Oxidatively Generated Damage to Cellular DNA by UVB and UVA Radiation ·. *Photochem Photobiol* 2015; **91**: 140–155.

43 Monaghan RM, Barnes RG, Fisher K, Andreou T, Rooney N, Poulin GB *et al.* A nuclear role for the respiratory enzyme CLK-1 in regulating mitochondrial stress responses and longevity. *Nat Cell Biol* 2015; **17**: 782–792.

44 Luo Z, Chen Y, Chen S, Welch W, Andresen B, Jose P *et al.* Comparison of inhibitors of superoxide generation in vascular smooth muscle cells. *Br J Pharmacol* 2009; **157**: 935–943.

45 Altieri F, Grillo C, Maceroni M, Chichiarelli S. DNA Damage and Repair: From Molecular Mechanisms to Health Implications. *Antioxid Redox Signal* 2008; **10**:

891–938.

46 Löbrich M, Shibata A, Beucher A, Fisher A, Ensminger M, Goodarzi AA *et al.* gammaH2AX foci analysis for monitoring DNA double-strand break repair: strengths, limitations and optimization. *Cell Cycle* 2010; **9**: 662–9.

47 Podhorecka M, Skladanowski A, Bozko P. H2AX Phosphorylation: Its Role in DNA Damage Response and Cancer Therapy. *J Nucleic Acids* 2010; **2010**: 1–9.

48 Rodríguez-Escudero I, Oliver MD, Andrés-Pons A, Molina M, Cid VJ, Pulido R. A comprehensive functional analysis of PTEN mutations: implications in tumor- and autism-related syndromes. *Hum Mol Genet* 2011; **20**: 4132–4142.

49 Beaumont KA, Shekar SL, Newton RA, James MR, Stow JL, Duffy DL *et al.* Receptor function, dominant negative activity and phenotype correlations for MC1R variant alleles. *Hum Mol Genet* 2007; **16**: 2249–2260.

50 Shahzad M, Sires Campos J, Tariq N, Herraiz Serrano C, Yousaf R, Jiménez-Cervantes C *et al.* Identification and functional characterization of natural human melanocortin 1 receptor mutant alleles in Pakistani population. *Pigment Cell Melanoma Res* 2015; **28**: 730–5.

51 Zanna PT, Sanchez-Laorden BL, Perez-Oliva AB, Turpin MC, Herraiz C, Jimenez-Cervantes C *et al.* Mechanism of dimerization of the human melanocortin 1 receptor. *Biochem Biophys Res Commun* 2008; **368**: 211–216.

52 Khaled M. Glycogen Synthase Kinase 3beta Is Activated by cAMP and Plays an Active Role in the Regulation of Melanogenesis. *J Biol Chem* 2002; **277**: 33690–33697.

53 Gharbi SI, Zvelebil MJ, Shuttleworth SJ, Hancox T, Saghir N, Timms JF *et al.* Exploring the specificity of the PI3K family inhibitor LY294002. *Biochem J* 2007; **404**: 15–21.

54 Jo H, Mondal S, Tan D, Nagata E, Takizawa S, Sharma AK *et al.* Small molecule-induced cytosolic activation of protein kinase Akt rescues ischemia-elicited neuronal death. *Proc Natl Acad Sci* 2012; **109**: 10581–10586.

55 Zhang T, Dutton-Regester K, Brown KM, Hayward NK. The genomic landscape of cutaneous melanoma. *Pigment Cell Melanoma Res* 2016; **29**: 266–283.

56 d'Ischia M, Wakamatsu K, Cicoira F, Di Mauro E, Garcia-Borron JC, Commo S *et al.* Melanins and melanogenesis: from pigment cells to human health and technological applications. *Pigment Cell Melanoma Res* 2015; **28**: 520–544.

57 Chedekel MR, Smith SK, Post PW, Pokora A, Vessell DL. Photodestruction of pheomelanin: role of oxygen. *Proc Natl Acad Sci U S A* 1978; **75**: 5395–9.

58 Felix CC, Hyde JS, Sarna T, Sealy RC. Melanin photoreactions in aerated media: electron spin resonance evidence for production of superoxide and

hydrogen peroxide. *Biochem Biophys Res Commun* 1978; **84**: 335–41.

59 Simon JD, Peles DN. The Red and the Black. *Acc Chem Res* 2010; **43**: 1452–1460.

60 Panzella L, Leone L, Greco G, Vitiello G, D'Errico G, Napolitano A *et al.* Red human hair pheomelanin is a potent pro-oxidant mediating UV-independent contributory mechanisms of melanomagenesis. *Pigment Cell Melanoma Res* 2014; **27**: 244–252.

61 Abdel-Malek ZA, Swope VB, Starner RJ, Koikov L, Cassidy P, Leachman S. Melanocortins and the melanocortin 1 receptor, moving translationally towards melanoma prevention. *Arch Biochem Biophys* 2014; **563**: 4–12.

62 Wolf Horrell EM, Boulanger MC, D'Orazio JA. Melanocortin 1 Receptor: Structure, Function, and Regulation. *Front Genet* 2016; **7**. doi:10.3389/fgene.2016.00095.

63 Robles-Espinoza CD, Roberts ND, Chen S, Leacy FP, Alexandrov LB, Pornputtapong N *et al.* Germline MC1R status influences somatic mutation burden in melanoma. *Nat Commun* 2016; **7**: 12064.

64 Johansson PA, Pritchard AL, Patch A-M, Wilmott JS, Pearson J V., Waddell N *et al.* Mutation load in melanoma is affected by *MC1R* genotype. *Pigment Cell Melanoma Res* 2017; **30**: 255–258.

65 Jarrett SG, Carter KM, D'Orazio JA. Paracrine regulation of melanocyte genomic stability: a focus on nucleotide excision repair. *Pigment Cell Melanoma Res* 2017; **30**: 284–293.

66 Abdel-Malek Z, Swope VB, Suzuki I, Akcali C, Harriger MD, Boyce ST *et al.* Mitogenic and melanogenic stimulation of normal human melanocytes by melanotropic peptides. *Proc Natl Acad Sci U S A* 1995; **92**: 1789–93.

67 Buscà R, Ballotti R. Cyclic AMP a key messenger in the regulation of skin pigmentation. *Pigment cell Res* 2000; **13**: 60–9.

68 Ito S, Wakamatsu K. Quantitative analysis of eumelanin and pheomelanin in humans, mice, and other animals: a comparative review. *Pigment cell Res* 2003; **16**: 523–31.

69 Slominski A, Tobin DJ, Shibahara S, Wortsman J. Melanin pigmentation in mammalian skin and its hormonal regulation. *Physiol Rev* 2004; **84**: 1155–1228.

70 Jarrett SG, Wolf Horrell EM, D'Orazio JA. AKAP12 mediates PKA-induced phosphorylation of ATR to enhance nucleotide excision repair. *Nucleic Acids Res* 2016; **44**: 10711–10726.

71 Hein A, Ouellette M, Yan Y. Radiation-induced signaling pathways that promote cancer cell survival (Review). *Int J Oncol* 2014. doi:10.3892/ijo.2014.2614.

72 Toulany M, Kehlbach R, Florczak U, Sak A, Wang S, Chen J *et al.* Targeting of AKT1 enhances radiation toxicity of human tumor cells by inhibiting DNA-PKcs-dependent DNA double-strand break repair. *Mol Cancer Ther* 2008; **7**: 1772–1781.

73 Habib SL, Yadav A, Kidane D, Weiss RH, Liang S. Novel protective mechanism of reducing renal cell damage in diabetes: Activation AMPK by AICAR increased NRF2/OGG1 proteins and reduced oxidative DNA damage. *Cell Cycle* 2016; **15**: 3048–3059.

74 Piao MJ, Kim KC, Choi J-Y, Choi J, Hyun JW. Silver nanoparticles down-regulate Nrf2-mediated 8-oxoguanine DNA glycosylase 1 through inactivation of extracellular regulated kinase and protein kinase B in human Chang liver cells. *Toxicol Lett* 2011; **207**: 143–148.

75 Janjetovic Z, Jarrett SG, Lee EF, Duprey C, Reiter RJ, Slominski AT. Melatonin and its metabolites protect human melanocytes against UVB-induced damage: Involvement of NRF2-mediated pathways. *Sci Rep* 2017; **7**: 1274.

76 Manning BD, Toker A. AKT/PKB Signaling: Navigating the Network. *Cell* 2017; **169**: 381–405.

77 O'Hayre M, Degese MS, Gutkind JS. Novel insights into G protein and G protein-coupled receptor signaling in cancer. *Curr Opin Cell Biol* 2014; **27**: 126–35.

78 Ahn J-H, McAvoy T, Rakhilin S V, Nishi A, Greengard P, Nairn AC. Protein kinase A activates protein phosphatase 2A by phosphorylation of the B56delta subunit. *Proc Natl Acad Sci U S A* 2007; **104**: 2979–84.

79 Cho E-A, Kim E-J, Kwak S-J, Juhnn Y-S. cAMP signaling inhibits radiation-induced ATM phosphorylation leading to the augmentation of apoptosis in human lung cancer cells. *Mol Cancer* 2014; **13**: 36.

80 Musante V, Li L, Kanyo J, Lam TT, Colangelo CM, Cheng SK *et al.* Reciprocal regulation of ARPP-16 by PKA and MAST3 kinases provides a cAMP-regulated switch in protein phosphatase 2A inhibition. *Elife* 2017; **6**. doi:10.7554/eLife.24998.

81 Yang J-L, Chen W-Y, Chen Y-P, Kuo C-Y, Chen S-D. Activation of GLP-1 Receptor Enhances Neuronal Base Excision Repair via PI3K-AKT-Induced Expression of Apurinic/Apyrimidinic Endonuclease 1. *Theranostics* 2016; **6**: 2015–2027.

82 Pan Y, Wang N, Xia P, Wang E, Guo Q, Ye Z. Inhibition of Rac1 ameliorates neuronal oxidative stress damage via reducing Bcl-2/Rac1 complex formation in mitochondria through PI3K/Akt/mTOR pathway. *Exp Neurol* 2018; **300**: 149–166.

83 Xu N, Lao Y, Zhang Y, Gillespie DA. Akt: a double-edged sword in cell

proliferation and genome stability. *J Oncol* 2012; **2012**: 951724.

84 Medrano EE, Im S, Yang F, Abdel-Malek ZA. Ultraviolet B light induces G1 arrest in human melanocytes by prolonged inhibition of retinoblastoma protein phosphorylation associated with long-term expression of the p21Waf-1/SDI-1/Cip-1 protein. *Cancer Res* 1995; **55**: 4047–52.

85 Hustedt N, Durocher D. The control of DNA repair by the cell cycle. *Nat Cell Biol* 2016; **19**: 1–9.

86 Perez Oliva AB, Fernendez LP, Detorre C, Herraiz C, Martinez-Escribano JA, Benitez J *et al.* Identification and functional analysis of novel variants of the human melanocortin 1 receptor found in melanoma patients. *Hum Mutat* 2009; **30**: 811–822.

87 Sánchez-Laorden BL, Sánchez-Más J, Martínez-Alonso E, Martínez-Menárguez J a, García-Borrón JC, Jiménez-Cervantes C. Dimerization of the human melanocortin 1 receptor: functional consequences and dominant-negative effects. *J Invest Dermatol* 2006; **126**: 172–181.

88 Herraiz C, Olivares C, Castejon-Grinan M, Abrisqueta M, Jimenez-Cervantes C, Garcia-Borron JC. Functional Characterization of MC1R-TUBB3 Intergenic Splice Variants of the Human Melanocortin 1 Receptor. *PLoS One* 2015; **10**: e0144757.

Supplementary Information accompanies the paper on the *Oncogene* website (http://www.nature.com/onc).

FIGURE LEGENDS

Figure 1. Effect of MC1R signalling on 8-oxodG levels induced by an oxidative challenge in HBL and A375 melanoma cells. (**a**) HBL were serum-deprived for 12 h and stimulated with 10^{-7} M NDP-MSH, 10^{-5} M FSK or $3x10^{-6}$ M dbcAMP, for 36 h with or without pretreatment with $2.5x10^{-3}$ M DDA for 1 h, or incubated with ebselen (40 μM, 36 h prior to and during the oxidative challenge), then treated with Luperox ($1.5x10^{-4}$ M, 30 min). After 8-oxodG immunostaining, samples were mounted with a medium from Dako (Glostrup, Denmark) and examined with a Leica laser scanning confocal microscope at 63x magnification (Leica GmbH, Wetzlar, Germany). Single plane images corresponding to Z positions of maximal DAPI signal were acquired and, nuclear 8-oxodG fluorescence signals were quantified calculating the pixel intensity in single cell nuclei relative to the nucleus area. This analysis was performed using software Qwin

(Leica Microsystems Ltd., Barcelona, Spain). At least 200 randomly selected cells were quantified. Representative confocal images of 8-oxodG immunostaining are shown (bar size: 50 μm), as well as quantitative analysis of nuclear 8-oxodG fluorescence intensity in each condition. (**b**) cAMP levels in HBL cells treated as above. (**c**) 8-oxodG and (**d**) cAMP levels in A375 cells treated as above (n = 3 independent experiments, error bars are mean±SEM, two-sided one-way ANOVA was used to generate p values, *p<0.05, **p<0.01, ***p<0.001, ****p<0.0001). (**e**) Activation of MITF gene expression by NDP-MSH in HBL cells, but not in A375 cells. Cells were serum-starved (12 h), then treated with NDP-MSH (10^{-7} M) for the times shown. mRNA was extracted, reverse-transcribed and MITF mRNA levels were compared by real-time PCR (n = 3, **p<0.01).

Figure 2. Effect of MC1R signalling on DNA strand breaks induced by Luperox in HBL and A375 melanoma cells. HBL (**a**) and A375 (**b**) melanoma cells were serum-deprived for 12 h and then stimulated with 10^{-7} M NDP-MSH for 36 h prior to Luperox treatment. Cells were fixed, permeabilized and stained for γH2AX (green). DAPI was used for nuclear staining (blue). Representative confocal images of γH2AX immunostaining obtained as described for 8-oxodG in Figure 1 (bar size: 5 μm) and the quantification of the relative intensity of γH2AX signals, performed as described for 8-oxodG staining in Figure 1, are shown below (n = 3 independent experiments, error bars, statistical analysis and p values as in Figure 1). Representative images of HBL (**c**) and A375 (**d**) cells treated as above, obtained at lower magnification (bar size 50 μm) to show homogenous staining of the cellular population. (**e**) Minor effect of NDP-MSH on cell cycle progression in HBL or A375 cells. MC1R-dependent protection against Luperox-induced DNA SBs in HBL (**f**) and A375 (**g**) cells. Comet assays were performed on cells treated with NDP-MSH, pharmacological cAMP-elevating agents or ebselen under the standard conditions described in Figure 1. Then, cells were harvested, suspended in PBS at 1 x 10^5 cells/ml, imbedded in low melting point agarose at 37º C at a ratio of 1:10 (v/v) and transferred onto microscope slides. After solidification at 4°C for 30 min, cells were lysed overnight, and DNA was unwound in alkaline electrophoresis solution, pH>13 (200 mM NaOH, 1 mM EDTA) for 20 min at RT. Slides were placed in an electrophoresis chamber and electrophoresis was performed in the same buffer at 25 V. Slides were then washed, dried for 30 min at 37º C and DNA was stained with Midori Green advanced. Quantitative analysis of at least 100 randomly selected comets was performed using a Leica fluorescence microscope and CASPLAB software. Histograms show the mean average of the tail moment of treated cells relative to untreated cells (n = 3 independent experiments, each one with at least 100 comets

analysed. Error bars, statistical analysis and p values as in Figure1). Representative images of comet tails acquired at 40X magnification are shown above each histogram.

Figure 3. Induction of antioxidant enzymes by αMSH in HBL and A375 melanoma cells. HBL melanoma cells (**a**), with or without pretreatment with $2.5x10^{-3}$ M DDA (hatched bars) or A375 melanoma cells (**b**) were stimulated with 10^{-7} M NDP-MSH at the indicated time points. Expression of *CAT* (orange bars), *SOD1* (blue) and *GPX1* (green) genes was estimated by quantitative real time PCR. Data are shown as relative expression of each enzyme in treated cells relative to untreated controls calculated using the $2^{-\Delta\Delta Ct}$ method. β-actin was used as endogenous normalizer. These data were compiled from three separate experiments performed in triplicate (n = 3, error bars are mean±SEM, statistical analysis and p values as in Figure 1). (**c**) Increased catalase expression in HBL melanoma cells stimulated with NDP-MSH. Representative immunoblots (top) and quantification (bottom) of catalase protein levels in HBL (left) and A375 melanoma cells (right) stimulated with 10^{-7} M NDP-MSH for the indicated times are shown. Quantification of 3 independent experiments using ERK2 signal as loading control is shown below the blots. Values were normalized to the 0 time-point (n = 3, error bars are mean±SEM, two-sided Student´s t test was used to generate p values, *p< 0.05). (**d**) Levels of SOD1 in HBL or A375 cells stimulated with 10^{-7} M NDP-MSH for the times shown, as analysed by Western blot. The number below each lane represents the normalized intensity of the SOD1 signals corrected for protein load (mean of two independent experiments). ERK2 was used as a control for protein load. (**e**) Intracellular ROS levels in Luperox-treated cells HBL and A375 cells. Cells were pretreated with NDP-MSH (10^{-7} M, 36 h), as indicated, then challenged with Luperox ($1.5x10^{-4}$ M, 30 min). Total ROS were measured with 2′7′dichlorodihydrofluorescein (n = 3, with 6 replicate wells for each experiment, error bars are mean±SEM, statistical analysis and p values as in Figure 1).

Figure 4. Effect of MC1R activation on the kinetics of oxidative DNA damage repair in human melanoma cells. HBL and A375 cells, as indicated, were pretreated or not with NDP-MSH (10^{-7} M, 36 h) during a short challenge with Luperox ($1.5x10^{-4}$ M, 10 min, 4ºC). Cells were quickly washed and further incubated for up to 15 min either in the absence (vehicle) or in the presence of NDP-MSH. Then cells were processed for 8-oxodG staining (panels a and b) or for single cell electrophoresis and comet assay (panels c, d) performed and quantified as specified in Figures 1 and 2, respectively. Control stands for cells that were not challenged with Luperox.

Figure 5. Lack of involvement of the ERK pathway in the protective effect of NDP-MSH in cells harboring *MC1R* variants. HBL (**a**) and A375 (**b**) melanoma cells were pretreated with the MEK1 inhibitor PD98059 ($5x10^{-5}$ M, 1h), then stimulated with NDP-MSH (10^{-7} M, 36 h) prior to a Luperox challenge ($1.5x10^{-4}$ M, 30 min). DNA breaks were analyzed by alkaline comet assay. Histograms show the mean average of the tail moment of treated cells relative to the tail moment of untreated cells (n = 3 independent experiments with at least 100 comets analysed in each case. Error bars, statistical analysis and p values as in Figure 1). Representative immunoblots ascertaining ERK inhibition by PD98059 are shown on the right along with the quantification of ERK phosphorylation levels relative to the control (n = 3, error bars as above).

Figure 6. AKT activation upon NDP-MSH stimulation of variant MC1R. Involvement in the protective effect of NDP-MSH. (**a**) Kinetics of AKT activation following stimulation of HBL and A375 cells with NDP-MSH. Cells were challenged with 10^{-7} M NDP-MSH for the times shown. Representative immunoblots for pAKT1/2/3 are shown for each cell line. Quantification of the intensity of pAKT signal relative to the control is shown below. Total AKT1/2/3 was used as loading control (n = 3, error bars are mean±SEM, *p<0.05, **p<0.01 ***p<0.001, ****p<0.0001, calculated with a two-sided Student´s t test). (**b**) Relationship between AKT activation and the cAMP pathway. HBL cells were pretreated with DDA ($2.5x10^{-3}$ M, 1 h) to block cAMP production, and conversely A375 melanoma cells were incubated with dbcAMP ($3x10^{-6}$ M, 30 min) to increase cAMP levels prior to stimulation with 10^{-7} M NDP-MSH for 60 and 90 min. Representative immunoblots and quantification of 3 independent blots for pAKT are shown (n = 3, error bars and statistics as in Figure 1). HBL (**c**) or A375 (**d**) melanoma cells were pretreated for 1 h with LY294002 ($2x10^{-5}$ M) and MK-2206 ($5x10^{-6}$ M), to block AKT stimulation. Then cells were stimulated with NDP-MSH (10^{-7} M, 36 h) prior to treatment with Luperox ($1.5x10^{-4}$ M, 30 min) and collected for comet assay. Cells were also treated with 10 μg/ml SC79, an activator of AKT, before the Luperox challenge. Histograms show the mean average of the tail moment of treated cells relative to the tail moment of untreated cells (n = 3 independent experiments with at least 100 comets scored in each case, error bars and statistical analysis as above). Representative immunoblots and their quantification for pAKT are shown to confirm AKT inhibition (n = 3 independent experiments, error bars, statistical analysis and p values as in Figure 1).

Figure 7. Proposed model for the differential coupling of WT and variant MC1R to different DNA repair pathways. In MC1R WT melanocytic cells, MC1R agonists induce

high cAMP levels that block AKT activation, so that cAMP-dependent DNA repair pathways are predominantly operative. In MC1R-variant melanocytes, failure to increase high cAMP levels enables AKT activation downstream of MC1R and AKT-dependent repair pathways would prevail.

cAMP-independent non-pigmentary actions of variant melanocortin 1 receptor: AKT-mediated activation of protective responses to oxidative DNA damage

María Castejón, Cecilia Herraiz[1], Conchi Olivares, Celia Jiménez-Cervantes and Jose Carlos García-Borrón

Department of Biochemistry, Molecular Biology and Immunology, School of Medicine, University of Murcia and Instituto Murciano de Investigacion Biosanitaria (IMIB).

[1] Corresponding author: Dr Cecilia Herraiz, ceciliahs@um.es. LAIB, Room 1.55. Campus de Ciencias de la Salud, Universidad de Murcia. Carretera Buenavista, s/n. 30120 El Palmar, Murcia, SPAIN.

Running title: cAMP-independent protective action of variant MC1R

Word count: Main text (Introduction, Results, Discussion and Methods): 4691 words (up to 4700 words allowed by the Editors)

Full text: 9484 words

Abstract

The melanocortin 1 receptor gene (*MC1R*), a well-established melanoma susceptibility gene, regulates the amount and type of melanin pigments formed within epidermal melanocytes. *MC1R* variants associated with increased melanoma risk promote production of photosensitizing pheomelanins as opposed to photoprotective eumelanins. Wild-type (WT) MC1R activates DNA repair and antioxidant defenses in a cAMP-dependent fashion. Since melanoma-associated *MC1R* variants are hypomorphic in cAMP signalling, these non-pigmentary actions are thought to be defective in *MC1R*-variant human melanoma cells and epidermal melanocytes, consistent with a higher mutation load in *MC1R*-variant melanomas. We compared induction of antioxidant enzymes and DNA damage responses in melanocytic cells of defined *MC1R* genotype. Increased expression of *catalase* (*CAT*) and *superoxide dismutase* (*SOD)* genes following MC1R activation was cAMP-dependent and required a WT MC1R genotype. Conversely, pretreatment of melanocytic cells with an MC1R agonist before an oxidative challenge with Luperox decreased i) accumulation of 8-oxo-7,8-dihydro-2'-deoxyguanine, a major product of oxidative DNA damage, ii) phosphorylation of histone H2AX, a marker of DNA double strand breaks and iii) formation of DNA breaks. These responses were comparable in cells WT for *MC1R* or harboring hypomorphic *MC1R* variants without detectable cAMP signalling. In *MC1R*-variant melanocytic cells, the DNA-protective responses were mediated by AKT. Conversely, in *MC1R*-WT melanocytic cells, high cAMP production downstream of MC1R blocked AKT activation and was responsible for inducing DNA repair. Accordingly, MC1R activation could promote repair of oxidative DNA damage by a cAMP-dependent pathway downstream of WT receptor, or via AKT in cells of variant *MC1R* genotype.

Keywords (3-6)

- melanocortin 1 receptor (MC1R)
- α melanocyte-stimulating hormone (α melanocortin; αMSH)
- oxidative DNA damage
- cAMP pathway
- AKT pathway
- melanoma

INTRODUCTION

The melanocortin 1 receptor (MC1R), a Gs protein-coupled receptor (GPCR) expressed by epidermal melanocytes, is critically involved in cutaneous responses to ultraviolet radiation (UVR)[1]. Solar UVR, the main external etiological factor for melanoma, causes DNA lesions directly or by oxidative processes triggered by UVR-induced reactive oxygen species (ROS). A causal link exists between UVR-induced DNA damage and skin carcinogenesis, particularly melanomagenesis[2–4]. Upon stimulation by keratinocyte-derived melanocortins, notably α melanocyte-stimulating hormone (αMSH), MC1R activates cAMP signalling to switch melanogenesis from basal synthesis of reddish pheomelanins to synthesis of darker eumelanins. Contrary to the well-established photoprotective effect of eumelanins, pheomelanins promote oxidative stress by UVR-dependent and independent mechanisms[5], thus acting as sensitizers that contribute to melanomagenesis[6]. Accordingly, dark-skinned individuals are less susceptible to sunburn and melanoma than people with pale skin.

Human *MC1R* (MIM#155555) is highly polymorphic, and almost 50% of individuals of Caucasian descent carry at least one variant allele[1,7,8]. Many *MC1R* polymorphisms are associated with pheomelanic pigmentation with red hair, fair skin, impaired tanning response to UVR and propensity to sunburn[9]. This phenotype, designated RHC, is also associated with skin cancer risk[10–12]. *MC1R* RHC alleles display hypomorphic signalling to the cAMP pathway[13–21]. The degree of functional impairment grossly correlates with penetrance, with strong R-type alleles such as R151C showing lower residual cAMP signalling than weaker "r-type" alleles[22].

Despite their photoprotective role, eumelanins only afford a moderate protection factor around 2-3 in darker-skinned individuals[23]. Moreover, a significant association of *MC1R* alleles and melanoma persists after stratification for pigmentation, pointing to pigment-independent actions of MC1R[24,25]. In *MC1R*-WT human melanocytes, αMSH enhances repair of UVR-induced cyclobutane pyrimidine dimers in a cAMP-dependent fashion[26,27]. Accordingly, it is believed that cAMP-dependent non-pigmentary actions including induction of antioxidant defenses and DNA repair contribute to the association of the *MC1R* genotype with melanoma[26–31].

Signalling downstream of MC1R is pleiotropic, with activation of mitogen-activated kinases ERK1/2 and the cAMP pathway[32]. In human melanocytes, ERK activation by MC1R relies on cAMP-independent transactivation of the cKIT tyrosine kinase receptor (RTK)[14,33,34]. Importantly, common R mutations impairing cAMP signalling have little effect on ERK activation downstream of MC1R[14,33,34], and their

possible effects on signalling to AKT remain largely unknown. Moreover, it has been shown that WT MC1R, but not several major RHC alleles, might prevent proteasomal degradation of PTEN[35], suggesting the possibility of a differential capability to activate AKT signalling. Both the ERKs[36–38] and AKT[39–41] play roles in DNA repair. Taken together, these observations suggest that variant *MC1R* with disrupted cAMP signalling might still be able to activate DNA damage responses. To test this hypothesis, we assessed MC1R-dependent protection against oxidative DNA damage in human melanoma cells (HMCs) and epidermal melanocytes of defined *MC1R* genotype. Given the relevance of oxidatively-generated DNA damage in the presence of pheomelanic pigmentation associated with *MC1R* variants[6], we focused on major oxidative lesions, namely 8-oxo-7,8-dihydro-2'-deoxyguanine (8-oxodG) and single or double strand breaks (SSBs or DSBs)[42]. We show the occurrence of cAMP-independent DNA repair mechanisms downstream of variant MC1R. We also show that variant MC1R activates AKT to promote DNA repair.

RESULTS

Induction of DNA repair downstream of variant MC1R

To investigate the effect of *MC1R* genotype on susceptibility to oxidative DNA damage, we first used two HMC lines, HBL and A375. HBL cells are WT for *MC1R*, *NRAS* and *BRAF*, whereas A375 cells carry the V600E *BRAF* mutation and are homozygous for the R151C *MC1R* variant (Supplementary Table S1). To mimic transient oxidative stress, cells were pulsed with tert-butyl hydroperoxide (Luperox) ($1.5x10^{-4}$ M, 30 min), used as a stable form of H_2O_2[43]. This treatment increased comparably ROS levels without significant effects on cell viability not only in A375 and HBL cells, but also in two other HMC lines (SKMEL28 and C8161) and Hermes human melanocytes (Supplementary Figures S1a, S1b). The oxidative challenge was performed with or without pretreatment (36 h) with the stable αMSH analogue NDP-MSH, the adenylyl cyclase (AC) activator forskolin (FSK) or the cell-permeable cAMP precursor dibutyryl-cAMP (dbcAMP). Then, Luperox-treated cells were stained for 8-oxodG, a major product of UVR-induced oxidative DNA damage. For *MC1R*-WT HBL cells, Luperox strongly increased 8-oxodG staining. This increase was abolished by the non-selective antioxidant ebselen[44] or by pretreatment with NDP-MSH, FSK or dbcAMP (Figure 1a and Supplementary Figure S1c). These treatments dramatically increased intracellular cAMP levels (Figure 1b). Furthermore, the AC inhibitor 2′,5′-dideoxyadenosine (DDA) blocked NDP-MSH or FSK-dependent cAMP production and decreased markedly their

protective effect (Figures 1a and 1b). Therefore, in WT *MC1R* HBL cells, the cAMP pathway contributed most of the MC1R-dependent reduction of ROS-induced oxidative DNA damage as assessed by 8-oxodG staining, in agreement with reports by others[29–31].

Pretreatment of *MC1R*-variant A375 cells with NDP-MSH also decreased 8-oxodG levels compared with treatment with Luperox alone (Figure 1c), but NDP-MSH failed to activate cAMP signalling as demonstrated by lack of stimulation of cAMP levels or *MITF* gene expression (Figure 1d and 1f). Thus, in A375 cells homozygous for the R151C allele, MC1R activation triggered a significant protective response most likely in a cAMP-independent manner. Interestingly, pretreatment of A375 HMCs with dbcAMP, but not FSK, achieved a strong increase in intracellular cAMP and had a strong protective effect against ROS-induced DNA oxidative damage (Figures 1c, 1d). This showed that the cAMP-activated pathway(s) responsible for protection against DNA oxidative insults remained operative in A375 cells.

Next, we analyzed variant MC1R-dependent protection against peroxide-generated DNA strand breaks (SBs). Exposure of cells to ROS such as peroxyl radicals increases SBs[45]. Whereas low micromolar peroxide concentrations mostly induce SSBs, relatively high concentrations such as those employed here also induce significant numbers of DSBs[46]. ROS-induced DSBs rapidly result in phosphorylation of histone H2AX**.** Phosphorylated H2AX (γH2AX) attracts repair factors to DSB sites, forming foci enriched in repair proteins[47]. In the same experimental conditions as for determination of 8-oxodG, Luperox treatment augmented γH2AX staining in HBL and A375 cells (Figures 2a, 2b). Preincubation with NDP-MSH prevented the increase in γH2AX staining in both cell lines, suggesting reduction of DSBs. The possibility that γH2AX foci, which are poorly induced by SSBs, might arise by conversion of such lesions to DSBs on passage of a replication fork in proliferating cells appeared unlikely, since a clear majority of cells exhibited extensive and similar staining (Figures 2c and 2d). Moreover, incubation with NDP-MSH, which reduced strongly γH2AX staining, had little effect on cell cycle progression (Figure 2e).

On the other hand, pretreatment of HBL cells with either FSK or dbcAMP also decreased the γH2AX signal. Conversely, only dbcAMP afforded protection to A375 cells (Supplementary Figure S2) but FSK was ineffective, in keeping with its previously observed inability to decrease peroxide-induced 8-oxodG or to activate significantly cAMP synthesis in these cells.

We wished to confirm MC1R-mediated reduction of DNA SBs in MC1R-variant A375 cells. To this end, we assessed oxidative DNA fragmentation using the alkaline comet assay. In HBL and A375 cells, NDP-MSH reduced Luperox-induced DNA SBs

(Figures 2f, 2g and Supplementary Table 2). As for γH2AX staining, preincubation with FSK decreased Luperox-generated SBs in HBL cells but not in A375 HMCs, whereas dbcAMP reduced SBs in both cell types. These data confirmed the involvement of cAMP- independent pathways in protection against oxidative DNA damage downstream of variant MC1R. Of note, the DNA damage repair response triggered by cAMP remained operative in these cell lines, as it could be evoked by dbcAMP.

To confirm the novel finding of cAMP-independent protective mechanisms downstream of variant MC1R, we analyzed three other melanocytic cell lines, SKMEL28 and C8161 HMCs and Hermes melanocytes. C8161 are heterozygotes for R151C *MC1R* and bear the V600E *BRAF* mutation (Supplementary Table S1). SKMEL28 cells carry the V600E *BRAF* mutation and the T167A *PTEN* mutation (Supplementary Figure S3a) causing partial loss-of-function with retention of significant phosphatase activity[48]. SKMEL28 cells are compound heterozygotes for *MC1R*, bearing the I155T R variant[49] and another variant allele, S83P, of unknown functional behaviour. We cloned the S83P variant for functional analysis. Upon stimulation with NDP-MSH, S83P MC1R expressed in HEK293T cells did not activate the cAMP pathway but retained full capacity to activate the ERKs (Supplementary Figure S3b-d). Therefore, S83P behaved as a strong R allele. We also found that Hermes melanocytes were *MC1R* heterozygotes carrying a natural variant allele coding for a $C275^{STOP}$ truncated protein. Cys275 is located within the 3rd extracellular loop of the receptor, and accordingly $C275^{STOP}$ lacks the complete 7th transmembrane fragment and cytosolic extension of the native receptor. We did not analyze this variant for function since our previous studies have shown that removal of the same regions in an artificial $C273^{STOP}$ mutant, or the C-terminal cytosolic extension in $Y298^{STOP}$ lead to complete loss of signalling to the cAMP pathway[50,51]. Treatment of SKMEL28, C8161 or Hermes cells with NDP-MSH did not increase cAMP levels (Supplementary Figure S4a). On the other hand, NDP-MSH transiently stimulated the ERKs in Hermes melanocytes (Supplementary Figure S4b).

Preincubation of C8161, SKMEL28 or Hermes cells with NDP-MSH comparably decreased the steady state levels of DNA SBs generated by Luperox (Supplementary Figure S5a). This suggested that the cAMP-independent protection against oxidative DNA fragmentation afforded by NDP-MSH in A375 cells was not an artefact of this cell type but was rather a general behaviour of MC1R-variant melanocytic cells. To further establish the ability of variant MC1R to protect against oxidative DNA damage, we transfected HEK293T cells with Flag epitope-labeled WT or R151C MC1R. At comparable expression levels, NDP-MSH elicited a similar protective response against

Luperox-induced DNA fragmentation, as estimated by comet assays (Supplementary Figure S5b).

The experiments described thus far were performed using a relatively long oxidative challenge (30 min) and a prolonged preincubation with NDP-MSH (36 h) that may allow for the induction of antioxidant enzymes. Therefore, the protective effect of MC1R activation could result from a combination of augmented clearance of oxidative lesions and decreased oxidative damage due to improved antioxidant defenses. To assess the relative contribution of these non-mutually exclusive mechanisms, we investigated the extent and kinetics of induction of antioxidant enzymes downstream of WT or variant MC1R. HBL or A375 cells were treated with NDP-MSH, and the expression of *catalase* (*CAT*), *superoxide dismutase* (*SOD1*) and *glutathione peroxidase* (*GPx1*) genes was assessed. For HBL cells, NDP-MSH caused a time-dependent induction of *CAT*, a faster stimulation of *SOD1* and a weaker increase in *GPx1* expression. These stimulatory effects were abolished by DDA-mediated inhibition of AC (Figure 3a). Moreover, upregulation of intracellular cAMP levels by FSK or dbcAMP also increased expression of *CAT*, *SOD1* and *GPx1* in HBL cells (Supplementary Figure S6a). These data were consistent with reports of cAMP-dependent upregulation of antioxidant enzymes downstream of WT MC1R[29–31]. Concerning A375 cells, NDP-MSH (Figure 3b) or FSK (Supplementary Figure S6b) had little effect on *CAT* expression and did not increase *GPx1* mRNA, whereas dbcAMP significantly stimulated *SOD* and *CAT* expression (Supplementary Figure S6b). Surprisingly, in A375 cells NDP-MSH and FSK upregulated potently and transiently *SOD1* expression, suggesting that in these cells signalling mechanisms different from the cAMP pathway could be responsible for *SOD1* upregulation downstream of MC1R.

We analyzed catalase and SOD1 protein levels upon MC1R stimulation with NDP-MSH for up to 48 h. We observed a significant induction of catalase in agonist-treated HBL cells, but A375 cells were unresponsive (Figure 3c). Expression of SOD1 did not change significantly in either cell type (Figure 3d). To find out whether upregulation of catalase led to a decreased ROS burden, we measured total ROS levels in NDP-MSH-treated cells. We found a trend towards lower ROS levels in NDP-MSH-stimulated cells that did not reach statistical significance (Figure 3e). Therefore, WT MC1R HMCs may cope with oxidative stress by induction of antioxidant enzymes in response to activation of the cAMP pathway. However, this effect would be small, and absent in *MC1R* variant HMCs. Accordingly, the protection against DNA damage in A375 cells treated with NDP-MSH most likely resulted from enhanced DNA repair.

To confirm activation of DNA repair pathways downstream of variant MC1R, we compared the rate of clearance of oxidative DNA lesions in control cells or cells

pretreated with NDP-MSH for 36 h. For this purpose, HBL and A375 HMCs kept on ice were challenged with Luperox for a shorter time (10 min), then quickly washed and incubated at 37ºC to follow the kinetics of 8-oxodG removal and comet tail clearance. In the absence of NDP-MSH, the intensity of 8-oxodG staining and the comet tail moments stayed constant for up to 15 min after removal of the oxidizing agent in HBL cells or even increased slightly in A375 cells (Figure 4). Conversely, NDP-MSH-treated cells showed a progressive clearance of 8-oxodG and a reduction of the comet tail moments, already noticeable after a 5 min recovery, thus confirming active DNA repair.

Involvement of AKT signalling in the protective effect of variant MC1R

We aimed at identifying MC1R-triggered, cAMP-independent signalling pathway(s) responsible for the protective effects of NDP-MSH in *MC1R*-variant cells. We showed previously that NDP-MSH triggers ERK activation by cAMP-independent transactivation of cKIT[14,33]. Thus, we assessed the effect of the ERK pathway inhibitor PD98059 on MC1R-induced DNA repair. In HBL cells, PD98059 inhibited effectively basal and NDP-MSH-induced ERK activity and decreased, but did not abolish, protection against oxidative DNA fragmentation afforded by NDP-MSH. Indeed, Luperox-challenged HBL cells pre-stimulated with NDP-MSH in the presence of PD98059 showed significant reductions of comet tail moments (Figure 5a). For A375 cells, NDP-MSH decreased comparably oxidative DNA SBs, in the presence or absence of PD98059 (Figure 5b), despite nearly complete ERK inhibition. We obtained similar results for SKMEL28 cells (Supplementary Figure S7). These observations ruled out ERK activation as responsible for protection against oxidative DNA fragmentation downstream of variant *MC1R*.

Next, we challenged HBL and A375 cells with NDP-MSH and compared the activatory AKT phosphorylation. NDP-MSH did not augment AKT phosphorylation in WT *MC1R* HBL cells but activated AKT in A375 cells (Figure 6a). We observed a comparable activation of AKT in NDP-MSH-treated SKMEL28, C8161 and Hermes cells, with peak levels at 60-90 min (Supplementary Figure S8a). Therefore, variant MC1R activated AKT efficiently, but AKT activation downstream of MC1R was undetectable in cells expressing WT MC1R. This suggested an inverse relationship between AKT activation and the cAMP pathway. Since high cAMP levels inhibit AKT in B16 mouse melanoma cells[52], we reasoned that a similar inhibition might occur in human cells. To test this possibility, we blocked AC activation with DDA in HBL cells, and we increased cAMP levels in A375 cells with dbcAMP. Then, we challenged cells with NDP-MSH and compared pAKT levels. DDA allowed activation of AKT downstream of MC1R in HBL cells, whereas elevation of cAMP in A375 melanoma

cells abolished AKT phosphorylation (Figure 6b). Similar results were obtained for SKMEL28, C8161 and Hermes cells (Supplementary Figure 8b).

Since AKT was activated downstream of variant MC1R, we checked its involvement in MC1R-dependent reduction of oxidative DNA damage. We blocked the AKT pathway with pharmacological inhibitors and analyzed comet tail moments in Luperox-pulsed cells. We used LY94002 and MK-2206 to block PI3K and AKT activation, respectively[53]. This treatment prevented AKT activation and abolished the protective action of NDP-MSH in A375 but not in HBL cells (Figures 6c, 6d and Supplementary Figure S9). Moreover, this treatment also blocked protection in C8161, SKMEL28 and Hermes cells (Supplementary Figure S8c-e). To confirm a protective effect of AKT signalling in MC1R-variant melanoma cells, the oxidative challenge was performed in cells pretreated with SC79, an agonist of the AKT pathway which binds to AKT to induce a conformation favorable for phosphorylation by upstream activatory kinases[54]. SC79 had no effect on tail moments in HBL cells, consistent with its inability to increase pAKT levels in these cells (Figure 6c). Conversely, SC79 activated AKT efficiently in A375 cells (Figure 6d) and reduced Luperox-induced comet tail moments. Again, we observed a similar behaviour in other melanocytic cells (Supplementary Figure S8c-e). Therefore, the PI3K/AKT pathway was involved in NDP-MSH-induced clearance of DNA SBs downstream of variant MC1R.

DISCUSSION

WT *MC1R* protects against melanomagenesis by a combination of pigmentation-dependent and independent mechanisms[1]. The main external etiologic factor for melanoma is solar UVR, which causes direct DNA damage through its UVB component, or ROS-induced lesions through less energetic UVA radiation[3,4,55] resulting in high mutational rates. The pigmentation-dependent component of *MC1R* protective action is accounted for by a switch from basal pheomelanogenesis to eumelanogenesis. Eumelanin is a photoprotective pigment owing to its absorption properties in the UVR spectrum and its free radical scavenging properties[56]. Conversely, pheomelanin is a photosensitizer promoting ROS production upon exposure to UVR[5,57–59], that can reduce the intracellular antioxidant pool even in the absence of UVR[60]. Accordingly, pheomelanins promote melanomagenesis in mice carrying a conditional *BRAF*-mutant allele[6]. Concerning non-pigmentary actions, WT MC1R signalling activates antioxidant enzymes[28,30] and DNA repair pathways[61,62]. Owing to this combination of pigment-dependent and -independent effects, the

mutation load in WT *MC1R* melanomas is lower compared with *MC1R*-variant melanomas[63–65].

MC1R triggers several signalling pathways, and most *MC1R* alleles associated with higher melanoma risk are not loss-of-function variants *sensu stricto,* since they activate the ERKs with an efficiency comparable with WT, despite impaired cAMP signalling[1,14,33,34]. The pheomelanogenesis/eumelanogenesis switch depends upon activation of the cAMP pathway [66–69]. Therefore, inefficient cAMP signalling accounts for the pigmentary component of the association of *MC1R* variants and melanoma risk. Moreover, cAMP signalling stimulates non-pigmentary protective responses, including activation of base and nucleotide excision repair (BER and NER)[29–31,70]. However, ERK and AKT signalling play important roles in the activation of cell cycle checkpoints in response to DNA damage and in the induction of DNA repair mechanisms[39,71]. Therefore, *MC1R* alleles unable to promote cAMP-dependent eumelanogenesis might still be able to trigger cAMP-independent non-pigmentary responses. Thus, we compared the response of HMCs of defined *MC1R* genotype to oxidative challenges mimicking UVA-induced oxidative stress.

We found that NDP-MSH reduced significantly oxidative DNA damage in human melanoma cells of WT or variant *MC1R* genotype, as shown by decreased steady-state levels of 8-oxodG, γH2AX foci and DNA SBs. In HBL cells expressing WT MC1R, this protective effect may be partially accounted for by increased antioxidant defenses, since a significant induction of catalase by NDP-MSH was detected. However, in A375 cells expressing the hypomorphic R151C MC1R variant, this protective effect occurred without induction of antioxidant enzymes, pointing to activation of DNA repair, which was confirmed by kinetic analysis of clearance of oxidative DNA lesions after short Luperox challenges. Therefore, our data showed that variant *MC1R* can activate DNA repair.

Since *MC1R*-variant melanocytic cells used in this study failed to activate the cAMP pathway downstream of MC1R, we looked for the signalling pathways involved in their pigment-independent protective action. In MC1R-variant cells, NDP-MSH decreased comparably Luperox-induced DNA fragmentation in the absence or presence of the MEK inhibitor PD98059 (Figure 5), thus ruling out involvement of ERK signalling in the DNA protective effect. On the other hand, NDP-MSH significantly activated AKT in cells of variant *MC1R* genetic background. AKT is directly involved in DNA repair processes[39,71], promoting non-homologous end joining (NHEJ)-mediated repair of DSBs after irradiation of cancer cells[72], and inducing the BER of oxidized bases through activation of nuclear factor erythroid 2-related factor 2 (Nrf2) and subsequent upregulation of 8-oxoguanine glycosylase 1 (OGG1)[73,74]. This mechanism

has been recently shown to account for the protection against UVB-induced damage afforded by melatonin treatment of cultured human melanocytes[75]. In keeping with the protective role of AKT in other cell types, the AKT activator SC79 decreased the number of DNA SBs in Luperox-treated *MC1R*-variant HMCs. Moreover, blocking AKT signalling with LY94002 and MK-2206 abolished variant *MC1R*-dependent activation of DNA repair. Notably, in melanoma cells WT for MC1R, neither NDP-MSH nor SC79 activated AKT. Conversely, blocking cAMP production in these cells with DDA rescued AKT activation downstream of MC1R. On the other hand, pharmacological elevation of cAMP levels in *MC1R* variant HMCs also blocked AKT activation downstream of MC1R (Figure 6). Therefore, cAMP inhibited AKT signalling in HMCs, as previously shown for mouse melanoma cells[52,69]. Consistent with lack of AKT activation downstream of WT MC1R, induction of protective responses by NDP-MSH was unaffected by LY94002 and MK-2206. Conversely, these responses were blocked by DDA and mimicked by FSK or dbcAMP, confirming their dependence on cAMP. However, our data do not exclude the possible occurrence of ERK-dependent SB repair in MC1R-WT cells. Accordingly, our results suggest a model whereby MC1R activation promotes protection against oxidative DNA damage at least by two mechanisms, one of them dependent on cAMP and operative in MC1R-WT cells, whereas the other would depend on AKT and would be restricted to *MC1R*-variant cells (Figure 7).

The pathway linking variant MC1R to AKT activation remains unclear. The level of active, phospho-AKT reflects the balance between the opposing actions of activatory kinases working in a phosphatidylinositol triphosphate (PIP_3)-PI3K-dependent manner on one hand, and dephosphorylation by PP2A or PHLPP phosphatases on the other[76]. In turn, PI3K-PIP_3 signaling is activated downstream of RTKs or GPCRs and is terminated by PTEN. In human melanocytes, MC1R activates the cKIT RTK[33], but treatment of A375 cells with the cKIT inhibitors AG1478 or dasatinib did not block AKT activation by NDP-MSH (data not shown). In turn, PI3K activation by GPCRs most often relies on G protein activation via release of βγ dimers from αβγ heterotrimers[77]. However, MC1R variants do not stimulate efficiently cAMP synthesis indicating that they do not achieve significant levels of G protein activation. Accordingly, AKT activation by variant MC1R might result from interference with an inhibitory phosphatase, rather than activation of upstream kinase(s). This possibility is consistent with the slow kinetics of AKT activation by NDP-MSH in MC1R-variant cells. Notably, in MSH-treated UV-irradiated melanocytes, WT MC1R recruits PTEN in an interaction that prevents PTEN ubiquitination by WWP2, thereby protecting the phosphatase from proteasomal degradation[35]. The resulting PTEN stabilization partially downregulates AKT signaling. Conversely, MC1R variants such as R151C interact poorly with PTEN,

allowing for PTEN degradation and higher AKT activity. On the other hand, cAMP can activate PP2A, leading to inactivation of AKT[78–80]. Accordingly, a differential regulation of the levels or activity of phosphatases might underlie the different effect of WT and variant MC1R on AKT. This possibility is currently under study.

Oxidative injury to guanine and SSBs are usually repaired by BER, whereas DSBs are cleared by homologous recombination (HR) or NHEJ[39,65]. Variant MC1R accelerates clearance of 8-oxodG, the DSB marker γH2AX and comet tails, and therefore it might stimulate BER as well as HR or NHEJ. Activation of BER downstream of WT MC1R has been demonstrated[29], but the MC1R-regulated genes/proteins responsible for this protective effect remain largely unknown. Notably, two key components of BER, OGG1 and apurinic apyrimidinic endonuclease 1 (APE-1/Ref-1) are induced in MSH-treated melanocytes[29], and the pathways accounting for these effects remain uncharacterized. The involvement of AKT is likely, since AKT activates APE-1/Ref-1 in other cell types[81] and also regulates OGG1 activity, although in this case both inhibition and activation were reported, suggesting cell-type or context-dependent effects[73,74,82]. The latter activation occurs via AKT-mediated induction of the nuclear factor Nrf2 in response to oxidative stress[73–75].

In summary, here we showed that AKT was activated downstream of variant MC1R in human melanocytic cells. This activation was blunted downstream of the WT receptor due to a suppressive effect of cAMP. We also showed that variant MC1R accelerated the AKT-dependent clearance of 8-oxodG and DNA SBs, implying that it activated BER and recombinational repair. It remains to be seen how these observations can be reconciled with higher mutation loads in melanomas of variant *MC1R* genetic background compared with *MC1R*-WT melanomas[63,64]. In this respect, several possibilities can be considered. Variant MC1R may not activate NER-mediated clearance of UVB-produced lesions such as cyclobutene pyrimidine dimers as effectively as WT. Moreover, the precise cAMP-dependent DNA repair pathways triggered by WT MC1R may not be the same as the AKT-dependent pathways activated by variant MC1R. AKT plays opposite roles in the two major types of NER by promoting transcription-coupled NER while inhibiting global genome NER[39]. Concerning repair of DSBs, AKT was shown to inhibit HR while activating NHEJ[39,83]. Importantly, NHEJ may be particularly important for DSB clearance in UVR-irradiated melanocytes, since UVR induces G1 cell cycle arrest[84] and HR is restricted to the S and G2 phases[85]. The possibility of a differential engagement of DSB repair pathways by WT and variant MC1R is currently under study. In any case, our demonstration of AKT-dependent DNA repair downstream of variant MC1R may be important for the

design of rational melanoma prevention treatments such as application of topical agents increasing cAMP levels in sun-exposed skin.

METHODS

Cell culture

Cell culture reagents were from Gibco (Gaithersburg, MD) or Gentaur (Kampenhout, Belgium). Melanoma cells and HEK293T cells were grown in DMEM with 10% fetal bovine serum (FBS). Hermes melanocytes were cultured in Melanocyte Medium-2 with 5% FBS and 10% Melanocyte Growth Supplement-PMA-free. Serum and supplements were removed 1 day before, and during each experiment.

Expression constructs and transfection

Flag-tagged WT and variant MC1R has been described[86]. S83P MC1R was obtained by site-directed mutagenesis with the QuikChange XL Site-Directed Mutagenesis kit (Agilent, Santa Clara, CA) using Flag-WT-MC1R as template. HEK293T cells were transfected with 0.15 or 0.3 µg of plasmid DNA/well for 24 or 12-well plates, respectively, using Lipofectamine 2000 (Invitrogen) and Opti-MEM (Gibco).

Analysis of *MC1R* and *PTEN* mutation status

MC1R and *PTEN* ORFs were amplified from cDNA obtained using SuperScript™ III First-Strand Synthesis System (Invitrogen) and sequenced from two different PCR reactions to confirm each mutation. See Supplementary Table 3 for details on amplification procedures.

Immunoblotting

Western blotting was performed as described[87] using antibodies summarized in Supplementary Table 4.

Functional assays

cAMP was determined using a commercial immunoassay from Arbor Assays (Eisenhower Place, Michigan, USA)[88].

Immunofluorescence, confocal microscopy and image quantification

For 8-oxodG staining, HBL and A375 cells fixed with methanol followed by acetone at -20° C were treated with 0.05N HCl (5 min, 4º C) and 100 µg/ml RNAse (1 h, 37° C). DNA was denatured *in situ* with 0.15 N NaOH in 70% EtOH. Cells were incubated in 5 µg/ml proteinase K for 10 min at 37° C, blocked with 5% goat serum and incubated with anti-8-oxodG (Trevigen, Gaithersburg, MD, USA), followed by an Alexa 488-conjugated secondary antibody (Molecular Probes, Invitrogen), and with DAPI (10 µg/ml, Invitrogen Life Technologies).

For γ-H2AX staining, HBL and A375 cells fixed with 4% *p*-formaldehyde, were permeabilized with 0.5% Triton-X 100 (v/v) and blocked with 5% BSA. Cells were

labeled with anti-γH2A.X (phospho-S139) monoclonal antibody (Abcam, Cambridge, UK), followed by an Alexa 488-conjugated secondary antibody. Images were analyzed using Qwin Software (Leica Microsystems Ltd., Barcelona, Spain).

Intracellular ROS assay

ROS levels were assessed with 2′7′dichlorodihydrofluorescein diacetate (Molecular Probes). Fluorescence was measured at 492 nm excitation and 517 nm emission and normalized for cell numbers with crystal violet.

Comet assay

The Alkaline Comet Assay was performed per the manufacturer's protocol (Trevigen). DNA was unwound by treatment in alkaline electrophoresis solution, pH>13 (200 mM NaOH, 1 mM EDTA) for 20 min, and stained with Midori Green advanced (Nippon genetics Europe, Düren, Germany). Images were taken using a Leica fluorescence microscope. Quantitative analysis of tail moments of at least 100 randomly selected comets per sample was performed using CASPLAB software (http://www.casp.of.pl).

Gene expression analysis by real-time PCR

Cells were serum-deprived at least 12 h before RNA extraction with RNeasy (QIAGEN, Hilden, Germany). One µg of RNA was reverse-transcribed using SuperScript® III. RT-PCR was performed using the Power SYBR Green PCR Master Mix (Applied Biosystem) on ABI 7500 Fast Real Time PCR System. β-actin was used as endogenous normalizer. See Supplementary Table 5 for primers sequences.

Statistical analysis

Experiments were performed with at least three biological replicates. The sample size was chosen using GRANMO (https://www.imim.es/ofertadeserveis/software-public/granmo/index.html) and is indicated in figure legends. No samples were excluded from any analyses. Subpopulations of cells were randomly assigned to treatments. Blind analysis was not performed in this study. Statistical significance was assessed using GraphPad Software (San Diego California, USA). Data met the assumptions of the test used. We used D'Angostino-Pearson omnibus normality test for Gaussian distribution. Unpaired two-tailed Student's t-test and one-way ANOVA with Tukey post-test for multiple comparisons were performed when variance among groups was not statistically different. Otherwise, we used one-way Kruskal-Wallis test. Results are expressed as mean±SEM. p values were calculated using two-sided tests.

ACKNOWLEDGEMENTS

Supported by grants SAF2015-67092-R from MINECO (Spain) and FEDER (European Community) and 19875/GERM/15 from Fundación Seneca, Comunidad Autónoma de

la Región de Murcia (CARM). M Castejón holds a pre-doctoral fellowship from the Fundación Seneca. Cecilia Herraiz was a Juan de la Cierva-Incorporación fellow of MINECO. We thank Prof G Ghanem, from the Free University of Brussels for gift of human melanoma cell lines and Prof Neptuno Rodríguez (University of Murcia) for Hermes melanocytes. We also thank Prof. J.L. Castejón for help with the statistical analysis of data, Dr. M. Abrisqueta for assistance in cell cycle analysis and Dr. A. López-Contreras for suggestions and critical reading of the manuscript.

CONFLICT OF INTEREST

The authors declared no conflict of interest.

REFERENCES

1 Garcia-Borron JC, Abdel-Malek Z, Jimenez-Cervantes C. MC1R, the cAMP pathway, and the response to solar UV: extending the horizon beyond pigmentation. *Pigment Cell Melanoma Res* 2014; **27**: 699–720.

2 Merlino G, Herlyn M, Fisher DE, Bastian BC, Flaherty KT, Davies MA *et al.* The state of melanoma: challenges and opportunities. *Pigment Cell Melanoma Res* 2016; **29**: 404–16.

3 Krauthammer M, Kong Y, Ha BH, Evans P, Bacchiocchi A, McCusker JP *et al.* Exome sequencing identifies recurrent somatic RAC1 mutations in melanoma. *Nat Genet* 2012; **44**: 1006–1014.

4 Hodis E, Watson IR, Kryukov G V, Arold ST, Imielinski M, Theurillat JP *et al.* A landscape of driver mutations in melanoma. *Cell* 2012; **150**: 251–263.

5 Napolitano A, Panzella L, Monfrecola G, d'Ischia M. Pheomelanin-induced oxidative stress: bright and dark chemistry bridging red hair phenotype and melanoma. *Pigment Cell Melanoma Res* 2014; **27**: 721–733.

6 Mitra D, Luo X, Morgan A, Wang J, Hoang MP, Lo J *et al.* An ultraviolet-radiation-independent pathway to melanoma carcinogenesis in the red hair/fair skin background. *Nature* 2012; **491**: 449–453.

7 Box NF, Wyeth JR, O'Gorman LE, Martin NG, Sturm RA. Characterization of melanocyte stimulating hormone receptor variant alleles in twins with red hair. *Hum Mol Genet* 1997; **6**: 1891–7.

8 Smith R, Healy E, Siddiqui S, Flanagan N, Steijlen PM, Rosdahl I *et al.* Melanocortin 1 Receptor Variants in an Irish Population. *J Invest Dermatol* 1998; **111**: 119–122.

9 Valverde P, Healy E, Jackson I, Rees JL, Thody a J. Variants of the melanocyte-stimulating hormone receptor gene are associated with red hair and

fair skin in humans. *Nat Genet* 1995; **11**: 328–330.

10 Davies JR, Randerson-Moor J, Kukalizch K, Harland M, Kumar R, Madhusudan S *et al.* Inherited variants in the MC1R gene and survival from cutaneous melanoma: a BioGenoMEL study. *Pigment Cell Melanoma Res* 2012; **25**: 384–394.

11 Dessinioti C, Antoniou C, Katsambas A, Stratigos AJ. Melanocortin 1 receptor variants: functional role and pigmentary associations. *Photochem Photobiol*; **87**: 978–87.

12 Scherer D, Kumar R. Genetics of pigmentation in skin cancer--a review. *Mutat Res* 2010; **705**: 141–153.

13 Frandberg PA, Doufexis M, Kapas S, Chhajlani V. Human pigmentation phenotype: a point mutation generates nonfunctional MSH receptor. *Biochem Biophys Res Commun* 1998; **245**: 490–492.

14 Herraiz C, Jimenez-Cervantes C, Zanna P, Garcia-Borron JC. Melanocortin 1 receptor mutations impact differentially on signalling to the cAMP and the ERK mitogen-activated protein kinase pathways. *FEBS Lett* 2009; **583**: 3269–3274.

15 Nakayama K, Soemantri A, Jin F, Dashnyam B, Ohtsuka R, Duanchang P *et al.* Identification of novel functional variants of the melanocortin 1 receptor gene originated from Asians. *Hum Genet* 2006; **119**: 322–330.

16 Newton RA, Smit SE, Barnes CC, Pedley J, Parsons PG, Sturm RA. Activation of the cAMP pathway by variant human MC1R alleles expressed in HEK and in melanoma cells. *Peptides* 2005; **26**: 1818–1824.

17 Ringholm A, Klovins J, Rudzish R, Phillips S, Rees JL, Schiöth HB. Pharmacological characterization of loss of function mutations of the human melanocortin 1 receptor that are associated with red hair. *J Invest Dermatol* 2004; **123**: 917–923.

18 Roberts DW, Newton RA, Leonard JH, Sturm RA. Melanocytes expressing MC1R polymorphisms associated with red hair color have altered MSH-ligand activated pigmentary responses in coculture with keratinocytes. *J Cell Physiol* 2008; **215**: 344–55.

19 Schiöth HB, Phillips SR, Rudzish R, Birch-Machin M a, Wikberg JE, Rees JL. Loss of function mutations of the human melanocortin 1 receptor are common and are associated with red hair. *Biochem Biophys Res Commun* 1999; **260**: 488–491.

20 Scott MC, Wakamatsu K, Ito S, Kadekaro AL, Kobayashi N, Groden J *et al.* Human melanocortin 1 receptor variants, receptor function and melanocyte response to UV radiation. *J Cell Sci* 2002; **115**: 2349–2355.

21 Sanchez-Laorden BL, Sanchez-Mas J, Martinez-Alonso E, Martinez-Menarguez JA, Garcia-Borron JC, Jimenez-Cervantes C. Dimerization of the human melanocortin 1 receptor: functional consequences and dominant-negative effects. *J Invest Dermatol* 2006; **126**: 172–181.

22 Garcia-Borron JC, Olivares C. Melanocortin 1 receptor and skin pathophysiology: beyond colour, much more than meets the eye. *Exp Dermatol* 2014; **23**: 387–388.

23 Fajuyigbe D, Young AR. The impact of skin colour on human photobiological responses. *Pigment Cell Melanoma Res* 2016; **29**: 607–618.

24 Bastiaens MT, ter Huurne J a, Kielich C, Gruis N a, Westendorp RG, Vermeer BJ *et al.* Melanocortin-1 receptor gene variants determine the risk of nonmelanoma skin cancer independently of fair skin and red hair. *Am J Hum Genet* 2001; **68**: 884–894.

25 Gerstenblith MR, Goldstein AM, Fargnoli MC, Peris K, Landi MT. Comprehensive evaluation of allele frequency differences of MC1R variants across populations. *Hum Mutat* 2007; **28**: 495–505.

26 Bohm M, Wolff I, Scholzen TE, Robinson SJ, Healy E, Luger TA *et al.* alpha-Melanocyte-stimulating hormone protects from ultraviolet radiation-induced apoptosis and DNA damage. *J Biol Chem* 2005; **280**: 5795–5802.

27 Kadekaro AL, Kavanagh R, Kanto H, Terzieva S, Hauser J, Kobayashi N *et al.* alpha-Melanocortin and endothelin-1 activate antiapoptotic pathways and reduce DNA damage in human melanocytes. *Cancer Res* 2005; **65**: 4292–4299.

28 Kadekaro AL, Leachman S, Kavanagh RJ, Swope V, Cassidy P, Supp D *et al.* Melanocortin 1 receptor genotype: an important determinant of the damage response of melanocytes to ultraviolet radiation. *FASEB J* 2010; **24**: 3850–3860.

29 Kadekaro AL, Chen J, Yang J, Chen S, Jameson J, Swope VB *et al.* Alpha-Melanocyte-Stimulating Hormone Suppresses Oxidative Stress through a p53-Mediated Signaling Pathway in Human Melanocytes. *Mol Cancer Res* 2012; **10**: 778–786.

30 Maresca V, Flori E, Bellei B, Aspite N, Kovacs D, Picardo M. MC1R stimulation by alpha-MSH induces catalase and promotes its re-distribution to the cell periphery and dendrites. *Pigment Cell Melanoma Res* 2010; **23**: 263–75.

31 Song X, Mosby N, Yang J, Xu A, Abdel-Malek Z, Kadekaro AL. alpha-MSH activates immediate defense responses to UV-induced oxidative stress in human melanocytes. *Pigment Cell Melanoma Res* 2009; **22**: 809–18.

32 Herraiz C, Garcia-Borron JC, Jiménez-Cervantes C, Olivares C. MC1R signaling. Intracellular partners and pathophysiological implications. *Biochim*

Biophys Acta - Mol Basis Dis 2017. doi:10.1016/j.bbadis.2017.02.027.

33 Herraiz C, Journe F, Abdel-Malek Z, Ghanem G, Jimenez-Cervantes C, Garcia-Borron JC. Signaling from the human melanocortin 1 receptor to ERK1 and ERK2 mitogen-activated protein kinases involves transactivation of cKIT. *Mol Endocrinol* 2011; **25**: 138–156.

34 Herraiz C, Journe F, Ghanem G, Jimenez-Cervantes C, Garcia-Borron JC. Functional status and relationships of melanocortin 1 receptor signaling to the cAMP and extracellular signal-regulated protein kinases 1 and 2 pathways in human melanoma cells. *Int J Biochem Cell Biol* 2012; **44**: 2244–2252.

35 Cao J, Wan L, Hacker E, Dai X, Lenna S, Jimenez-Cervantes C *et al.* MC1R is a potent regulator of PTEN after UV exposure in melanocytes. *Mol Cell* 2013; **51**: 409–422.

36 Cohen-Armon M. PARP-1 activation in the ERK signaling pathway. *Trends Pharmacol Sci* 2007; **28**: 556–60.

37 Wei F, Yan J, Tang D. Extracellular signal-regulated kinases modulate DNA damage response - a contributing factor to using MEK inhibitors in cancer therapy. *Curr Med Chem* 2011; **18**: 5476–82.

38 Hawkins AJ, Golding SE, Khalil A, Valerie K. DNA double-strand break - induced pro-survival signaling. *Radiother Oncol* 2011; **101**: 13–7.

39 Liu Q, Turner KM, Alfred Yung WK, Chen K, Zhang W. Role of AKT signaling in DNA repair and clinical response to cancer therapy. *Neuro Oncol* 2014; **16**: 1313–1323.

40 Toulany M, Rodemann HP. Phosphatidylinositol 3-kinase/Akt signaling as a key mediator of tumor cell responsiveness to radiation. *Semin Cancer Biol* 2015; **35**: 180–190.

41 Singh P, Dar MS, Dar MJ. p110α and p110β isoforms of PI3K signaling: are they two sides of the same coin? *FEBS Lett* 2016; **590**: 3071–3082.

42 Cadet J, Douki T, Ravanat J-L. Oxidatively Generated Damage to Cellular DNA by UVB and UVA Radiation ·. *Photochem Photobiol* 2015; **91**: 140–155.

43 Monaghan RM, Barnes RG, Fisher K, Andreou T, Rooney N, Poulin GB *et al.* A nuclear role for the respiratory enzyme CLK-1 in regulating mitochondrial stress responses and longevity. *Nat Cell Biol* 2015; **17**: 782–792.

44 Luo Z, Chen Y, Chen S, Welch W, Andresen B, Jose P *et al.* Comparison of inhibitors of superoxide generation in vascular smooth muscle cells. *Br J Pharmacol* 2009; **157**: 935–943.

45 Altieri F, Grillo C, Maceroni M, Chichiarelli S. DNA Damage and Repair: From Molecular Mechanisms to Health Implications. *Antioxid Redox Signal* 2008; **10**:

891–938.

46 Löbrich M, Shibata A, Beucher A, Fisher A, Ensminger M, Goodarzi AA *et al.* gammaH2AX foci analysis for monitoring DNA double-strand break repair: strengths, limitations and optimization. *Cell Cycle* 2010; **9**: 662–9.

47 Podhorecka M, Skladanowski A, Bozko P. H2AX Phosphorylation: Its Role in DNA Damage Response and Cancer Therapy. *J Nucleic Acids* 2010; **2010**: 1–9.

48 Rodríguez-Escudero I, Oliver MD, Andrés-Pons A, Molina M, Cid VJ, Pulido R. A comprehensive functional analysis of PTEN mutations: implications in tumor- and autism-related syndromes. *Hum Mol Genet* 2011; **20**: 4132–4142.

49 Beaumont KA, Shekar SL, Newton RA, James MR, Stow JL, Duffy DL *et al.* Receptor function, dominant negative activity and phenotype correlations for MC1R variant alleles. *Hum Mol Genet* 2007; **16**: 2249–2260.

50 Shahzad M, Sires Campos J, Tariq N, Herraiz Serrano C, Yousaf R, Jiménez-Cervantes C *et al.* Identification and functional characterization of natural human melanocortin 1 receptor mutant alleles in Pakistani population. *Pigment Cell Melanoma Res* 2015; **28**: 730–5.

51 Zanna PT, Sanchez-Laorden BL, Perez-Oliva AB, Turpin MC, Herraiz C, Jimenez-Cervantes C *et al.* Mechanism of dimerization of the human melanocortin 1 receptor. *Biochem Biophys Res Commun* 2008; **368**: 211–216.

52 Khaled M. Glycogen Synthase Kinase 3beta Is Activated by cAMP and Plays an Active Role in the Regulation of Melanogenesis. *J Biol Chem* 2002; **277**: 33690–33697.

53 Gharbi SI, Zvelebil MJ, Shuttleworth SJ, Hancox T, Saghir N, Timms JF *et al.* Exploring the specificity of the PI3K family inhibitor LY294002. *Biochem J* 2007; **404**: 15–21.

54 Jo H, Mondal S, Tan D, Nagata E, Takizawa S, Sharma AK *et al.* Small molecule-induced cytosolic activation of protein kinase Akt rescues ischemia-elicited neuronal death. *Proc Natl Acad Sci* 2012; **109**: 10581–10586.

55 Zhang T, Dutton-Regester K, Brown KM, Hayward NK. The genomic landscape of cutaneous melanoma. *Pigment Cell Melanoma Res* 2016; **29**: 266–283.

56 d'Ischia M, Wakamatsu K, Cicoira F, Di Mauro E, Garcia-Borron JC, Commo S *et al.* Melanins and melanogenesis: from pigment cells to human health and technological applications. *Pigment Cell Melanoma Res* 2015; **28**: 520–544.

57 Chedekel MR, Smith SK, Post PW, Pokora A, Vessell DL. Photodestruction of pheomelanin: role of oxygen. *Proc Natl Acad Sci U S A* 1978; **75**: 5395–9.

58 Felix CC, Hyde JS, Sarna T, Sealy RC. Melanin photoreactions in aerated media: electron spin resonance evidence for production of superoxide and

hydrogen peroxide. *Biochem Biophys Res Commun* 1978; **84**: 335–41.

59 Simon JD, Peles DN. The Red and the Black. *Acc Chem Res* 2010; **43**: 1452–1460.

60 Panzella L, Leone L, Greco G, Vitiello G, D'Errico G, Napolitano A *et al.* Red human hair pheomelanin is a potent pro-oxidant mediating UV-independent contributory mechanisms of melanomagenesis. *Pigment Cell Melanoma Res* 2014; **27**: 244–252.

61 Abdel-Malek ZA, Swope VB, Starner RJ, Koikov L, Cassidy P, Leachman S. Melanocortins and the melanocortin 1 receptor, moving translationally towards melanoma prevention. *Arch Biochem Biophys* 2014; **563**: 4–12.

62 Wolf Horrell EM, Boulanger MC, D'Orazio JA. Melanocortin 1 Receptor: Structure, Function, and Regulation. *Front Genet* 2016; **7**. doi:10.3389/fgene.2016.00095.

63 Robles-Espinoza CD, Roberts ND, Chen S, Leacy FP, Alexandrov LB, Pornputtapong N *et al.* Germline MC1R status influences somatic mutation burden in melanoma. *Nat Commun* 2016; **7**: 12064.

64 Johansson PA, Pritchard AL, Patch A-M, Wilmott JS, Pearson J V., Waddell N *et al.* Mutation load in melanoma is affected by *MC1R* genotype. *Pigment Cell Melanoma Res* 2017; **30**: 255–258.

65 Jarrett SG, Carter KM, D'Orazio JA. Paracrine regulation of melanocyte genomic stability: a focus on nucleotide excision repair. *Pigment Cell Melanoma Res* 2017; **30**: 284–293.

66 Abdel-Malek Z, Swope VB, Suzuki I, Akcali C, Harriger MD, Boyce ST *et al.* Mitogenic and melanogenic stimulation of normal human melanocytes by melanotropic peptides. *Proc Natl Acad Sci U S A* 1995; **92**: 1789–93.

67 Buscà R, Ballotti R. Cyclic AMP a key messenger in the regulation of skin pigmentation. *Pigment cell Res* 2000; **13**: 60–9.

68 Ito S, Wakamatsu K. Quantitative analysis of eumelanin and pheomelanin in humans, mice, and other animals: a comparative review. *Pigment cell Res* 2003; **16**: 523–31.

69 Slominski A, Tobin DJ, Shibahara S, Wortsman J. Melanin pigmentation in mammalian skin and its hormonal regulation. *Physiol Rev* 2004; **84**: 1155–1228.

70 Jarrett SG, Wolf Horrell EM, D'Orazio JA. AKAP12 mediates PKA-induced phosphorylation of ATR to enhance nucleotide excision repair. *Nucleic Acids Res* 2016; **44**: 10711–10726.

71 Hein A, Ouellette M, Yan Y. Radiation-induced signaling pathways that promote cancer cell survival (Review). *Int J Oncol* 2014. doi:10.3892/ijo.2014.2614.

72 Toulany M, Kehlbach R, Florczak U, Sak A, Wang S, Chen J *et al.* Targeting of AKT1 enhances radiation toxicity of human tumor cells by inhibiting DNA-PKcs-dependent DNA double-strand break repair. *Mol Cancer Ther* 2008; **7**: 1772–1781.

73 Habib SL, Yadav A, Kidane D, Weiss RH, Liang S. Novel protective mechanism of reducing renal cell damage in diabetes: Activation AMPK by AICAR increased NRF2/OGG1 proteins and reduced oxidative DNA damage. *Cell Cycle* 2016; **15**: 3048–3059.

74 Piao MJ, Kim KC, Choi J-Y, Choi J, Hyun JW. Silver nanoparticles down-regulate Nrf2-mediated 8-oxoguanine DNA glycosylase 1 through inactivation of extracellular regulated kinase and protein kinase B in human Chang liver cells. *Toxicol Lett* 2011; **207**: 143–148.

75 Janjetovic Z, Jarrett SG, Lee EF, Duprey C, Reiter RJ, Slominski AT. Melatonin and its metabolites protect human melanocytes against UVB-induced damage: Involvement of NRF2-mediated pathways. *Sci Rep* 2017; **7**: 1274.

76 Manning BD, Toker A. AKT/PKB Signaling: Navigating the Network. *Cell* 2017; **169**: 381–405.

77 O'Hayre M, Degese MS, Gutkind JS. Novel insights into G protein and G protein-coupled receptor signaling in cancer. *Curr Opin Cell Biol* 2014; **27**: 126–35.

78 Ahn J-H, McAvoy T, Rakhilin S V, Nishi A, Greengard P, Nairn AC. Protein kinase A activates protein phosphatase 2A by phosphorylation of the B56delta subunit. *Proc Natl Acad Sci U S A* 2007; **104**: 2979–84.

79 Cho E-A, Kim E-J, Kwak S-J, Juhnn Y-S. cAMP signaling inhibits radiation-induced ATM phosphorylation leading to the augmentation of apoptosis in human lung cancer cells. *Mol Cancer* 2014; **13**: 36.

80 Musante V, Li L, Kanyo J, Lam TT, Colangelo CM, Cheng SK *et al.* Reciprocal regulation of ARPP-16 by PKA and MAST3 kinases provides a cAMP-regulated switch in protein phosphatase 2A inhibition. *Elife* 2017; **6**. doi:10.7554/eLife.24998.

81 Yang J-L, Chen W-Y, Chen Y-P, Kuo C-Y, Chen S-D. Activation of GLP-1 Receptor Enhances Neuronal Base Excision Repair via PI3K-AKT-Induced Expression of Apurinic/Apyrimidinic Endonuclease 1. *Theranostics* 2016; **6**: 2015–2027.

82 Pan Y, Wang N, Xia P, Wang E, Guo Q, Ye Z. Inhibition of Rac1 ameliorates neuronal oxidative stress damage via reducing Bcl-2/Rac1 complex formation in mitochondria through PI3K/Akt/mTOR pathway. *Exp Neurol* 2018; **300**: 149–166.

83 Xu N, Lao Y, Zhang Y, Gillespie DA. Akt: a double-edged sword in cell

proliferation and genome stability. *J Oncol* 2012; **2012**: 951724.

84 Medrano EE, Im S, Yang F, Abdel-Malek ZA. Ultraviolet B light induces G1 arrest in human melanocytes by prolonged inhibition of retinoblastoma protein phosphorylation associated with long-term expression of the p21Waf-1/SDI-1/Cip-1 protein. *Cancer Res* 1995; **55**: 4047–52.

85 Hustedt N, Durocher D. The control of DNA repair by the cell cycle. *Nat Cell Biol* 2016; **19**: 1–9.

86 Perez Oliva AB, Fernendez LP, Detorre C, Herraiz C, Martinez-Escribano JA, Benitez J *et al.* Identification and functional analysis of novel variants of the human melanocortin 1 receptor found in melanoma patients. *Hum Mutat* 2009; **30**: 811–822.

87 Sánchez-Laorden BL, Sánchez-Más J, Martínez-Alonso E, Martínez-Menárguez J a, García-Borrón JC, Jiménez-Cervantes C. Dimerization of the human melanocortin 1 receptor: functional consequences and dominant-negative effects. *J Invest Dermatol* 2006; **126**: 172–181.

88 Herraiz C, Olivares C, Castejon-Grinan M, Abrisqueta M, Jimenez-Cervantes C, Garcia-Borron JC. Functional Characterization of MC1R-TUBB3 Intergenic Splice Variants of the Human Melanocortin 1 Receptor. *PLoS One* 2015; **10**: e0144757.

Supplementary Information accompanies the paper on the *Oncogene* website (http://www.nature.com/onc).

FIGURE LEGENDS

Figure 1. Effect of MC1R signalling on 8-oxodG levels induced by an oxidative challenge in HBL and A375 melanoma cells. (**a**) HBL were serum-deprived for 12 h and stimulated with 10^{-7} M NDP-MSH, 10^{-5} M FSK or $3x10^{-6}$ M dbcAMP, for 36 h with or without pretreatment with $2.5x10^{-3}$ M DDA for 1 h, or incubated with ebselen (40 μM, 36 h prior to and during the oxidative challenge), then treated with Luperox ($1.5x10^{-4}$ M, 30 min). After 8-oxodG immunostaining, samples were mounted with a medium from Dako (Glostrup, Denmark) and examined with a Leica laser scanning confocal microscope at 63x magnification (Leica GmbH, Wetzlar, Germany). Single plane images corresponding to Z positions of maximal DAPI signal were acquired and, nuclear 8-oxodG fluorescence signals were quantified calculating the pixel intensity in single cell nuclei relative to the nucleus area. This analysis was performed using software Qwin

(Leica Microsystems Ltd., Barcelona, Spain). At least 200 randomly selected cells were quantified. Representative confocal images of 8-oxodG immunostaining are shown (bar size: 50 μm), as well as quantitative analysis of nuclear 8-oxodG fluorescence intensity in each condition. (**b**) cAMP levels in HBL cells treated as above. (**c**) 8-oxodG and (**d**) cAMP levels in A375 cells treated as above (n = 3 independent experiments, error bars are mean±SEM, two-sided one-way ANOVA was used to generate p values, *p<0.05, **p<0.01, ***p<0.001, ****p<0.0001). (**e**) Activation of MITF gene expression by NDP-MSH in HBL cells, but not in A375 cells. Cells were serum-starved (12 h), then treated with NDP-MSH (10^{-7} M) for the times shown. mRNA was extracted, reverse-transcribed and MITF mRNA levels were compared by real-time PCR (n = 3, **p<0.01).

Figure 2. Effect of MC1R signalling on DNA strand breaks induced by Luperox in HBL and A375 melanoma cells. HBL (**a**) and A375 (**b**) melanoma cells were serum-deprived for 12 h and then stimulated with 10^{-7} M NDP-MSH for 36 h prior to Luperox treatment. Cells were fixed, permeabilized and stained for γH2AX (green). DAPI was used for nuclear staining (blue). Representative confocal images of γH2AX immunostaining obtained as described for 8-oxodG in Figure 1 (bar size: 5 μm) and the quantification of the relative intensity of γH2AX signals, performed as described for 8-oxodG staining in Figure 1, are shown below (n = 3 independent experiments, error bars, statistical analysis and p values as in Figure 1). Representative images of HBL (**c**) and A375 (**d**) cells treated as above, obtained at lower magnification (bar size 50 μm) to show homogenous staining of the cellular population. (**e**) Minor effect of NDP-MSH on cell cycle progression in HBL or A375 cells. MC1R-dependent protection against Luperox-induced DNA SBs in HBL (**f**) and A375 (**g**) cells. Comet assays were performed on cells treated with NDP-MSH, pharmacological cAMP-elevating agents or ebselen under the standard conditions described in Figure 1. Then, cells were harvested, suspended in PBS at 1 x 10^5 cells/ml, imbedded in low melting point agarose at 37º C at a ratio of 1:10 (v/v) and transferred onto microscope slides. After solidification at 4°C for 30 min, cells were lysed overnight, and DNA was unwound in alkaline electrophoresis solution, pH>13 (200 mM NaOH, 1 mM EDTA) for 20 min at RT. Slides were placed in an electrophoresis chamber and electrophoresis was performed in the same buffer at 25 V. Slides were then washed, dried for 30 min at 37º C and DNA was stained with Midori Green advanced. Quantitative analysis of at least 100 randomly selected comets was performed using a Leica fluorescence microscope and CASPLAB software. Histograms show the mean average of the tail moment of treated cells relative to untreated cells (n = 3 independent experiments, each one with at least 100 comets

analysed. Error bars, statistical analysis and p values as in Figure1). Representative images of comet tails acquired at 40X magnification are shown above each histogram.

Figure 3. Induction of antioxidant enzymes by αMSH in HBL and A375 melanoma cells. HBL melanoma cells (**a**), with or without pretreatment with $2.5x10^{-3}$ M DDA (hatched bars) or A375 melanoma cells (**b**) were stimulated with 10^{-7} M NDP-MSH at the indicated time points. Expression of *CAT* (orange bars), *SOD1* (blue) and *GPX1* (green) genes was estimated by quantitative real time PCR. Data are shown as relative expression of each enzyme in treated cells relative to untreated controls calculated using the $2^{-\Delta\Delta Ct}$ method. β-actin was used as endogenous normalizer. These data were compiled from three separate experiments performed in triplicate (n = 3, error bars are mean±SEM, statistical analysis and p values as in Figure 1). (**c**) Increased catalase expression in HBL melanoma cells stimulated with NDP-MSH. Representative immunoblots (top) and quantification (bottom) of catalase protein levels in HBL (left) and A375 melanoma cells (right) stimulated with 10^{-7} M NDP-MSH for the indicated times are shown. Quantification of 3 independent experiments using ERK2 signal as loading control is shown below the blots. Values were normalized to the 0 time-point (n = 3, error bars are mean±SEM, two-sided Student´s t test was used to generate p values, *p< 0.05). (**d**) Levels of SOD1 in HBL or A375 cells stimulated with 10^{-7} M NDP-MSH for the times shown, as analysed by Western blot. The number below each lane represents the normalized intensity of the SOD1 signals corrected for protein load (mean of two independent experiments). ERK2 was used as a control for protein load. (**e**) Intracellular ROS levels in Luperox-treated cells HBL and A375 cells. Cells were pretreated with NDP-MSH (10^{-7} M, 36 h), as indicated, then challenged with Luperox ($1.5x10^{-4}$ M, 30 min). Total ROS were measured with 2′7′dichlorodihydrofluorescein (n = 3, with 6 replicate wells for each experiment, error bars are mean±SEM, statistical analysis and p values as in Figure 1).

Figure 4. Effect of MC1R activation on the kinetics of oxidative DNA damage repair in human melanoma cells. HBL and A375 cells, as indicated, were pretreated or not with NDP-MSH (10^{-7} M, 36 h) during a short challenge with Luperox ($1.5x10^{-4}$ M, 10 min, 4ºC). Cells were quickly washed and further incubated for up to 15 min either in the absence (vehicle) or in the presence of NDP-MSH. Then cells were processed for 8-oxodG staining (panels a and b) or for single cell electrophoresis and comet assay (panels c, d) performed and quantified as specified in Figures 1 and 2, respectively. Control stands for cells that were not challenged with Luperox.

Figure 5. Lack of involvement of the ERK pathway in the protective effect of NDP-MSH in cells harboring *MC1R* variants. HBL (**a**) and A375 (**b**) melanoma cells were pretreated with the MEK1 inhibitor PD98059 ($5x10^{-5}$ M, 1h), then stimulated with NDP-MSH (10^{-7} M, 36 h) prior to a Luperox challenge ($1.5x10^{-4}$ M, 30 min). DNA breaks were analyzed by alkaline comet assay. Histograms show the mean average of the tail moment of treated cells relative to the tail moment of untreated cells (n = 3 independent experiments with at least 100 comets analysed in each case. Error bars, statistical analysis and p values as in Figure 1). Representative immunoblots ascertaining ERK inhibition by PD98059 are shown on the right along with the quantification of ERK phosphorylation levels relative to the control (n = 3, error bars as above).

Figure 6. AKT activation upon NDP-MSH stimulation of variant MC1R. Involvement in the protective effect of NDP-MSH. (**a**) Kinetics of AKT activation following stimulation of HBL and A375 cells with NDP-MSH. Cells were challenged with 10^{-7} M NDP-MSH for the times shown. Representative immunoblots for pAKT1/2/3 are shown for each cell line. Quantification of the intensity of pAKT signal relative to the control is shown below. Total AKT1/2/3 was used as loading control (n = 3, error bars are mean±SEM, *p<0.05, **p<0.01 ***p<0.001, ****p<0.0001, calculated with a two-sided Student´s t test). (**b**) Relationship between AKT activation and the cAMP pathway. HBL cells were pretreated with DDA ($2.5x10^{-3}$ M, 1 h) to block cAMP production, and conversely A375 melanoma cells were incubated with dbcAMP ($3x10^{-6}$ M, 30 min) to increase cAMP levels prior to stimulation with 10^{-7} M NDP-MSH for 60 and 90 min. Representative immunoblots and quantification of 3 independent blots for pAKT are shown (n = 3, error bars and statistics as in Figure 1). HBL (**c**) or A375 (**d**) melanoma cells were pretreated for 1 h with LY294002 ($2x10^{-5}$ M) and MK-2206 ($5x10^{-6}$ M), to block AKT stimulation. Then cells were stimulated with NDP-MSH (10^{-7} M, 36 h) prior to treatment with Luperox ($1.5x10^{-4}$ M, 30 min) and collected for comet assay. Cells were also treated with 10 μg/ml SC79, an activator of AKT, before the Luperox challenge. Histograms show the mean average of the tail moment of treated cells relative to the tail moment of untreated cells (n = 3 independent experiments with at least 100 comets scored in each case, error bars and statistical analysis as above). Representative immunoblots and their quantification for pAKT are shown to confirm AKT inhibition (n = 3 independent experiments, error bars, statistical analysis and p values as in Figure 1).

Figure 7. Proposed model for the differential coupling of WT and variant MC1R to different DNA repair pathways. In MC1R WT melanocytic cells, MC1R agonists induce

high cAMP levels that block AKT activation, so that cAMP-dependent DNA repair pathways are predominantly operative. In MC1R-variant melanocytes, failure to increase high cAMP levels enables AKT activation downstream of MC1R and AKT-dependent repair pathways would prevail.

Figure 1

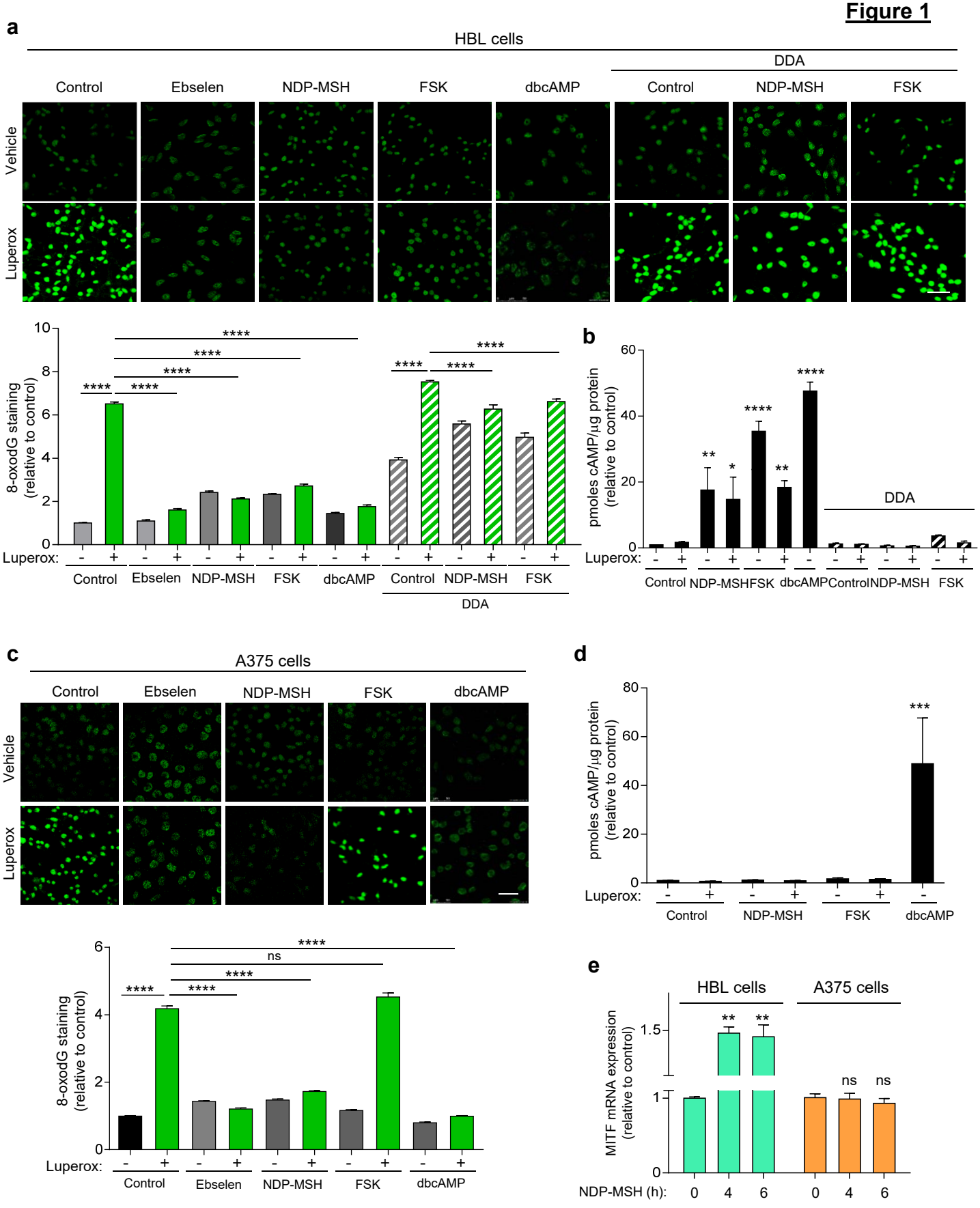
a
HBL cells
DDA
Control
Ebselen
NDP-MSH
FSK
dbcAMP
Control
NDP-MSH
FSK
Vehicle
Luperox
8-oxodG staining (relative to control)
Luperox:
Control
Ebselen
NDP-MSH
FSK
dbcAMP
Control
NDP-MSH
FSK
DDA
b
pmoles cAMP/µg protein (relative to control)
Luperox:
Control
NDP-MSH
FSK
dbcAMP
Control
NDP-MSH
FSK
DDA
c
A375 cells
Control
Ebselen
NDP-MSH
FSK
dbcAMP
Vehicle
Luperox
8-oxodG staining (relative to control)
ns
Luperox:
Control
Ebselen
NDP-MSH
FSK
dbcAMP
d
pmoles cAMP/µg protein (relative to control)
Luperox:
Control
NDP-MSH
FSK
dbcAMP
e
HBL cells
A375 cells
MITF mRNA expression (relative to control)
ns
NDP-MSH (h):
0
4
6
0
4
6

Figure 2

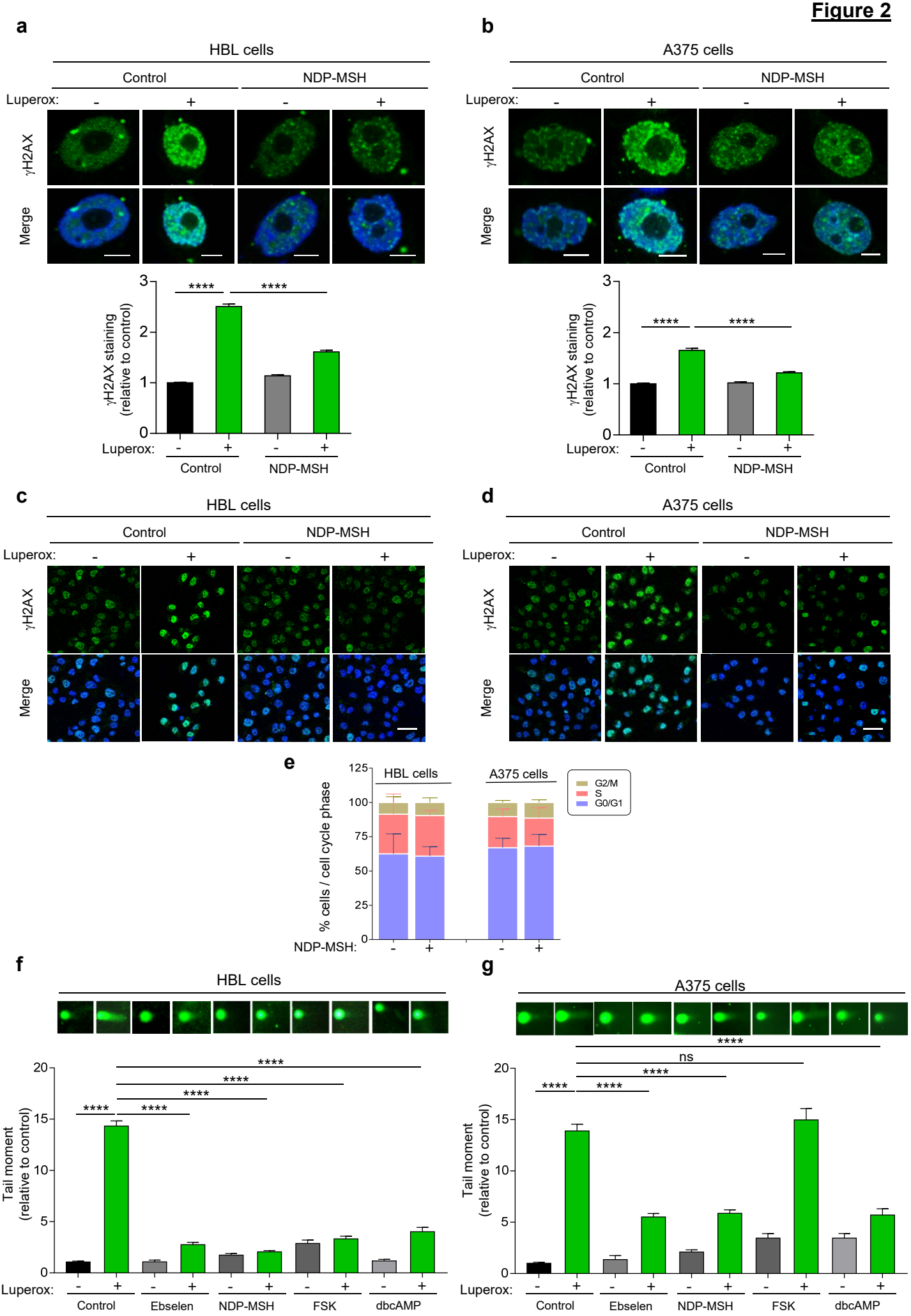
a
HBL cells
Control
NDP-MSH
Luperox:
γH2AX
Merge
γH2AX staining (relative to control)
****
b
A375 cells
c
HBL cells
d
A375 cells
e
HBL cells
A375 cells
% cells / cell cycle phase
G2/M
S
G0/G1
NDP-MSH:
f
HBL cells
Tail moment (relative to control)
Control
Ebselen
NDP-MSH
FSK
dbcAMP
g
A375 cells
ns

Figure 3

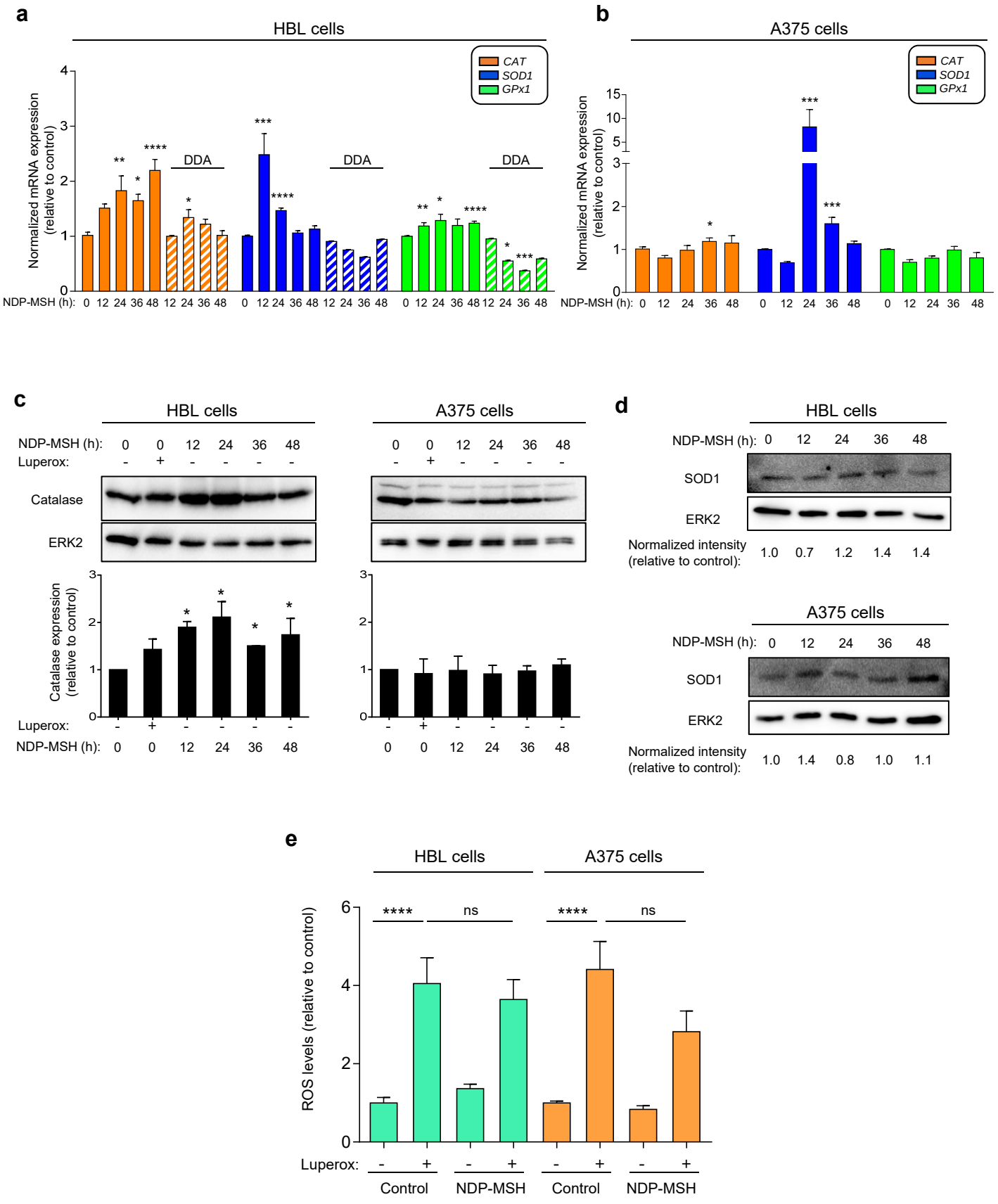
a
HBL cells
CAT
SOD1
GPx1
Normalized mRNA expression (relative to control)
DDA
DDA
DDA
NDP-MSH (h): 0 12 24 36 48 12 24 36 48 0 12 24 36 48 12 24 36 48 0 12 24 36 48 12 24 36 48
b
A375 cells
CAT
SOD1
GPx1
Normalized mRNA expression (relative to control)
NDP-MSH (h): 0 12 24 36 48 0 12 24 36 48 0 12 24 36 48
c
HBL cells
A375 cells
NDP-MSH (h): 0 0 12 24 36 48
Luperox: - + - - - -
Catalase
ERK2
Catalase expression (relative to control)
Luperox: - + - - - -
NDP-MSH (h): 0 0 12 24 36 48
d
HBL cells
NDP-MSH (h): 0 12 24 36 48
SOD1
ERK2
Normalized intensity (relative to control): 1.0 0.7 1.2 1.4 1.4
A375 cells
NDP-MSH (h): 0 12 24 36 48
SOD1
ERK2
Normalized intensity (relative to control): 1.0 1.4 0.8 1.0 1.1
e
HBL cells
A375 cells
**** ns **** ns
ROS levels (relative to control)
Luperox: - + - + - + - +
Control NDP-MSH Control NDP-MSH

Figure 4

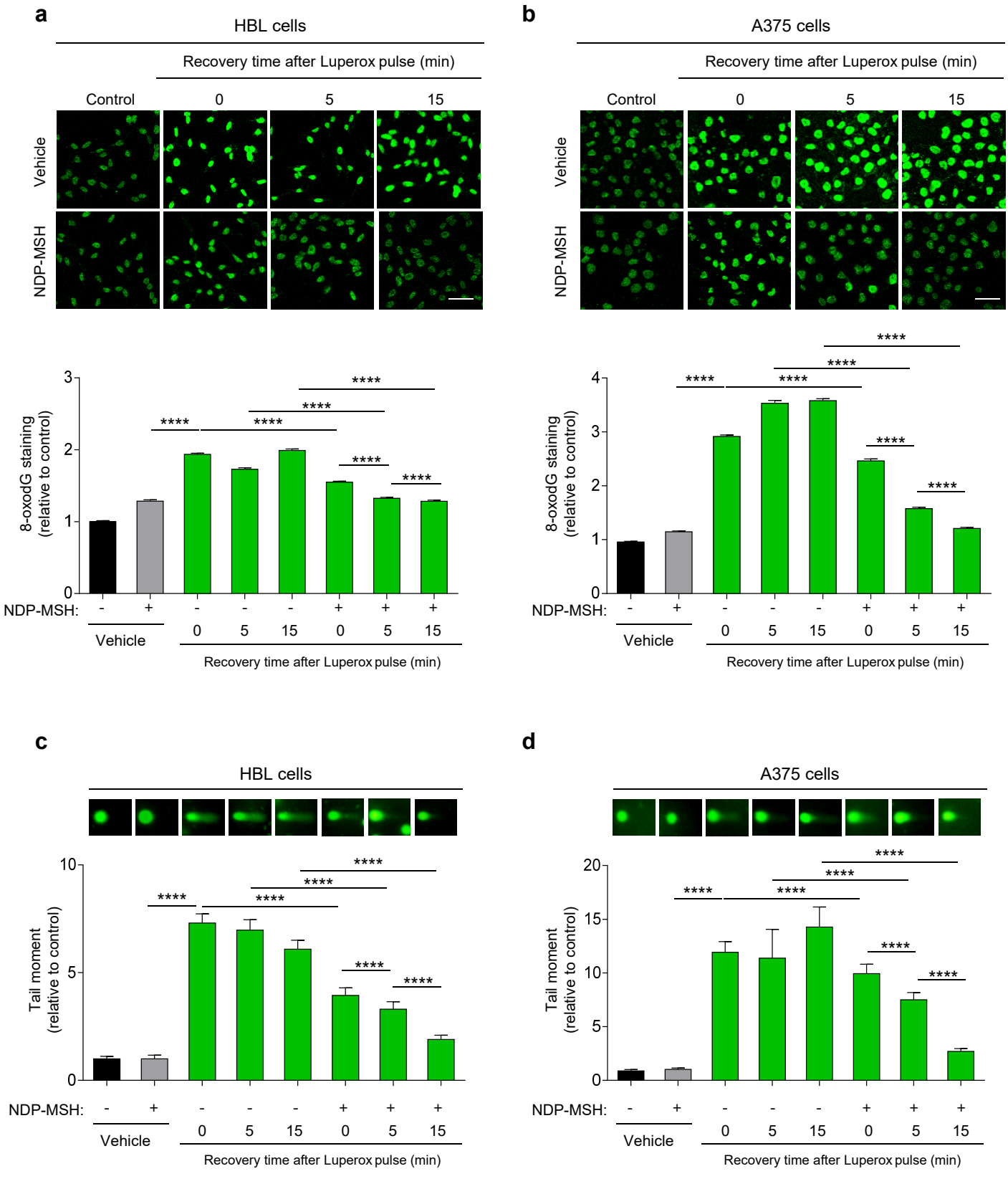
a
HBL cells
Recovery time after Luperox pulse (min)
Control
0
5
15
Vehicle
NDP-MSH
8-oxodG staining (relative to control)
NDP-MSH:
Vehicle
Recovery time after Luperox pulse (min)
b
A375 cells
c
HBL cells
Tail moment (relative to control)
d
A375 cells
****

Figure 5

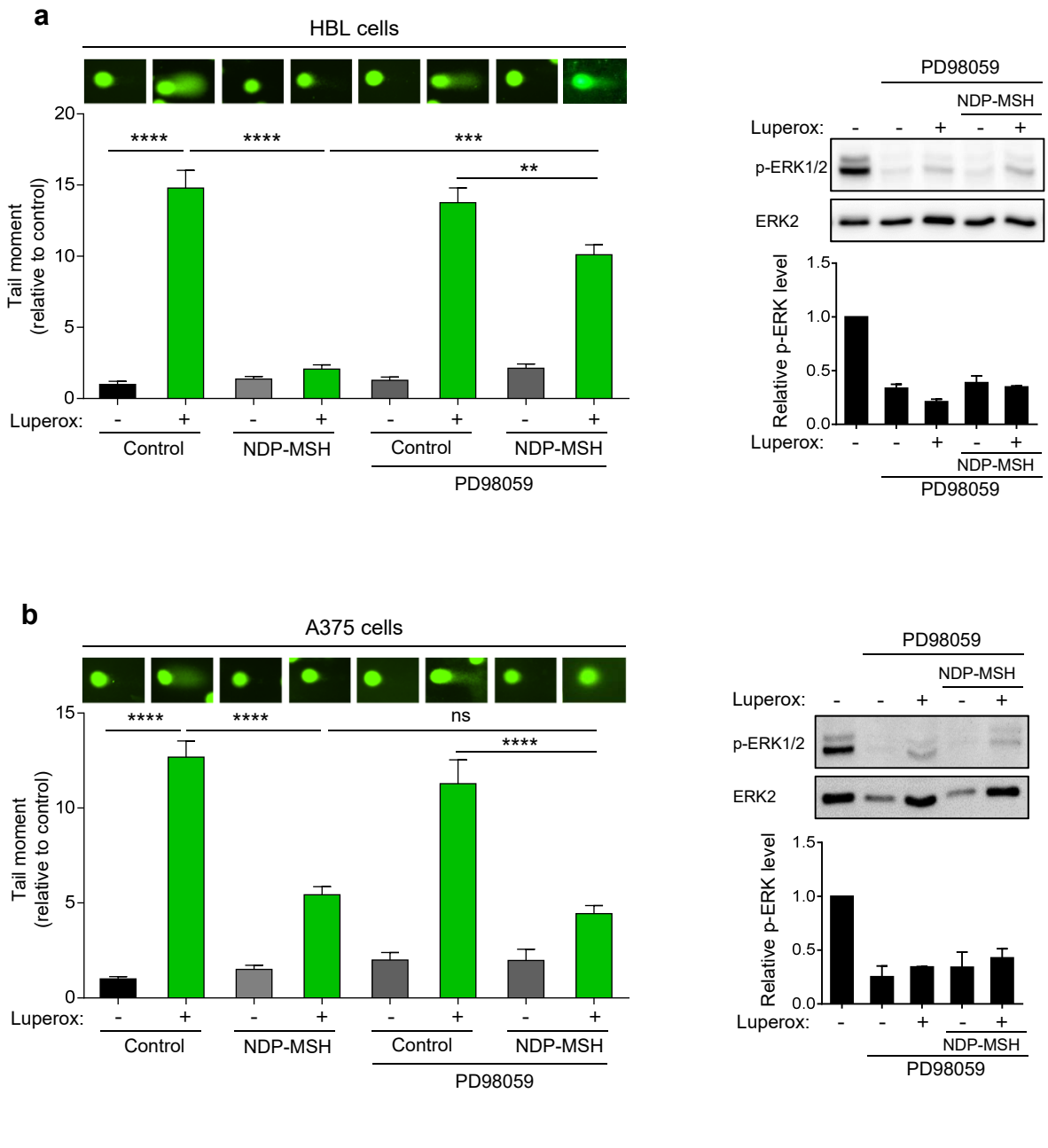
a
HBL cells
Tail moment (relative to control)
20
15
10
5
0
****
****
***
**
Luperox: - + - + - + - +
Control
NDP-MSH
Control
NDP-MSH
PD98059
PD98059
NDP-MSH
Luperox: - - + - +
p-ERK1/2
ERK2
Relative p-ERK level
1.5
1.0
0.5
0.0
Luperox: - - + - +
NDP-MSH
PD98059
b
A375 cells
Tail moment (relative to control)
15
10
5
0
****
****
ns
****
Luperox: - + - + - + - +
Control
NDP-MSH
Control
NDP-MSH
PD98059
PD98059
NDP-MSH
Luperox: - - + - +
p-ERK1/2
ERK2
Relative p-ERK level
1.5
1.0
0.5
0.0
Luperox: - - + - +
NDP-MSH
PD98059

Figure 6

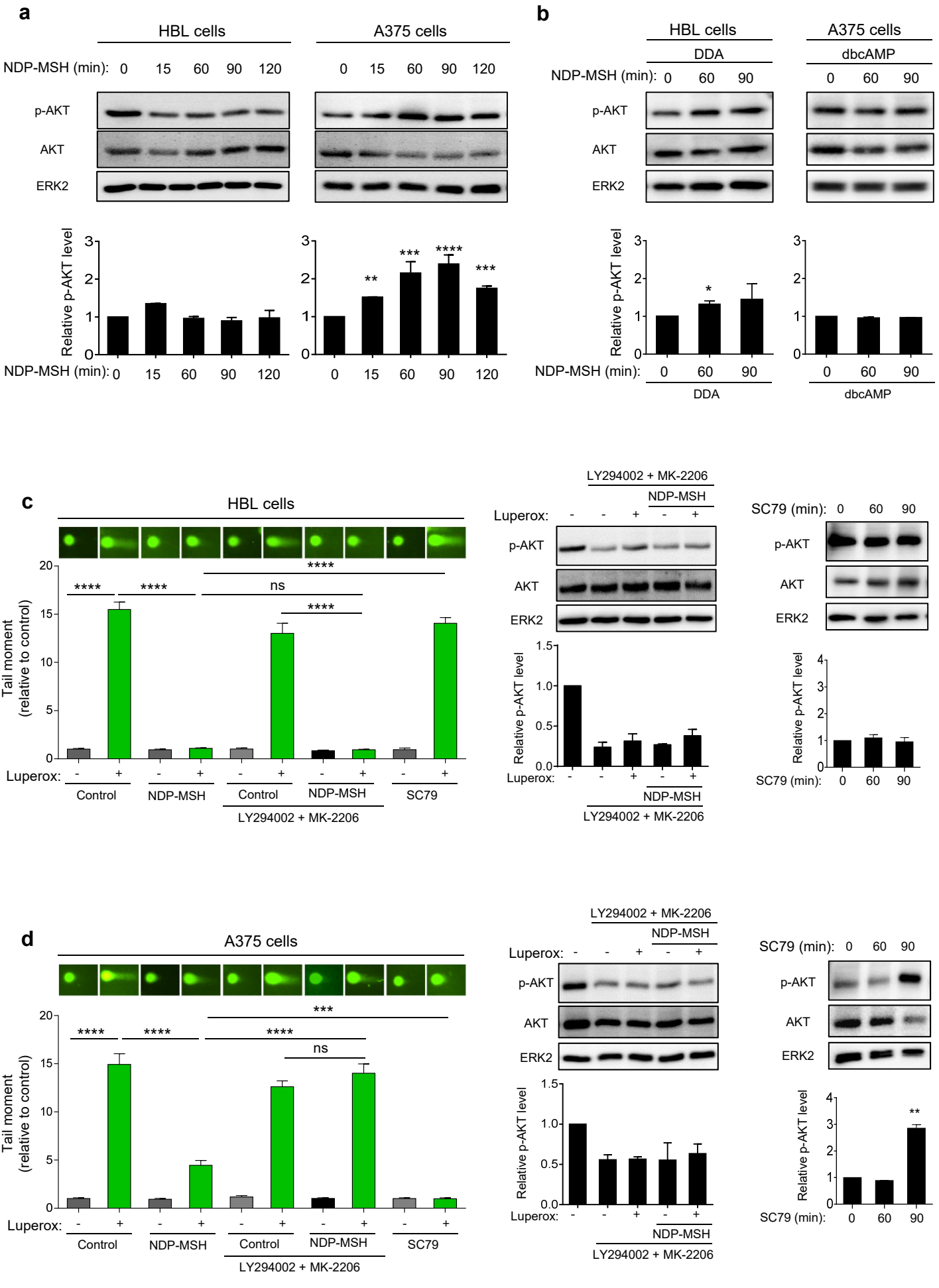
a
HBL cells
A375 cells
NDP-MSH (min): 0 15 60 90 120
p-AKT
AKT
ERK2
Relative p-AKT level
b
HBL cells
A375 cells
DDA
dbcAMP
NDP-MSH (min): 0 60 90
c
HBL cells
Tail moment (relative to control)
Luperox:
Control
NDP-MSH
SC79
LY294002 + MK-2206
ns
SC79 (min): 0 60 90
d
A375 cells

Figure 7

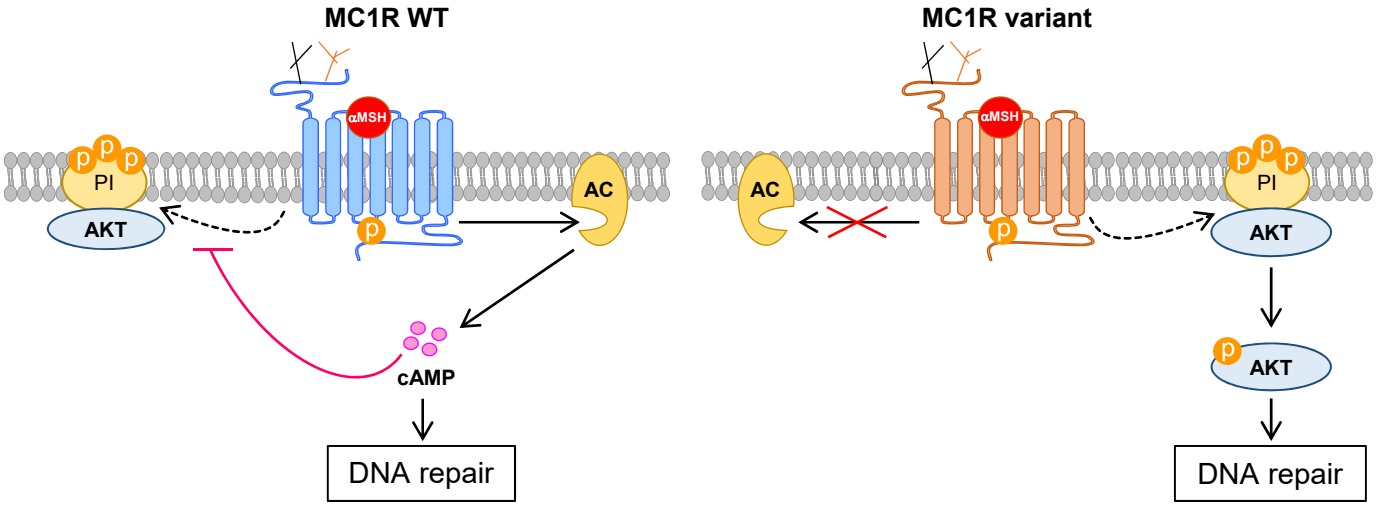
MC1R WT
αMSH
PI
AKT
AC
cAMP
DNA repair
MC1R variant
αMSH
AC
PI
AKT
AKT
DNA repair